https://doi.org/10.5194/acp-2020-973
Preprint. Discussion started: 20 October 2020

Atmospheric Chemistry and Physics Discussions

Reactive species formed upon interaction of water with fine particulate matter from remote forest and polluted urban air

Haijie Tong[1*], Fobang Liu[1,2], Alexander Filippi[1], Jake Wilson[1], Andrea M. Arangio[1,3], Yun Zhang[4], Siyao Yue[5,6,7], Steven Lelieveld[1], Fangxia Shen[1,8], Helmi-Marja K. Keskinen[9,10], Jing Li[11], Haoxuan Chen[11], Ting Zhang[11], Thorsten Hoffmann[4], Pingqing Fu[7], William H. Brune[12], Tuukka Petäjä[9], Markku Kulmala[9], Maosheng Yao[11], Thomas Berkemeier[1], Manabu Shiraiwa[13], Ulrich Pöschl[1]

[1] Multiphase Chemistry Department, Max Planck Institute for Chemistry, 55128 Mainz, Germany
[2] School of Chemical and Biomolecular Engineering, Georgia Institute of Technology, Atlanta, Georgia 30332, USA
[3] École polytechnique fédérale de Lausanne, Lausanne 1015, Switzerland
[4] Institute of Inorganic and Analytical Chemistry, Johannes Gutenberg University, 55128 Mainz, Germany
[5] State Key Laboratory of Atmospheric Boundary Layer Physics and Atmospheric Chemistry, Institute of Atmospheric Physics, Chinese Academy of Sciences, Beijing, 100029, China
[6] College of Earth and Planetary Sciences, University of Chinese Academy of Sciences, Beijing, 100049, China
[7] Institute of Surface-Earth System Science, Tianjin University, Tianjin, 300072, China
[8] School of Space and Environment, Beihang University, Beijing, 100191, China
[9] Institute for Atmospheric and Earth System Research / Physics, Faculty of Science, University of Helsinki, P.O. Box 64, FIN-00014, Helsinki, Finland
[10] Hyytiälä Forestry Field Station, Hyytiäläntie 124, FI-35500 Korkeakoski, Finland
[11] College of Environmental Sciences and Engineering, Peking University, Beijing, 100871, China
[12] Department of Meteorology, Pennsylvania State University, University Park, Pennsylvania 16802, United States
[13] Department of Chemistry, University of California, Irvine, California 92697-2025, USA

[*] *Correspondence to*: Haijie Tong (h.tong@mpic.de)

https://doi.org/10.5194/acp-2020-973
Preprint. Discussion started: 20 October 2020

Atmospheric Chemistry and Physics Discussions

Abstract

Interaction of water with fine particulate matter leads to the formation of reactive species (RS) that may influence the aging, properties, and health effects of atmospheric aerosols. In this study, we explore the RS yields of fine PM from remote forest (Hyytiälä, Finland) and polluted urban air (Mainz, Germany and Beijing, China) and relate these yields to different chemical constituents and reaction mechanisms. Ultrahigh-resolution mass spectrometry was used to characterize organic aerosol composition, electron paramagnetic resonance (EPR) spectroscopy with a spin-trapping technique was used to determine the concentrations $^{\bullet}OH$, $O_2^{\bullet-}$, and carbon- or oxygen-centered organic radicals, and a fluorometric assay was used to quantify H_2O_2 concentration. The mass-specific yields of radicals were lower for sampling sites with higher concentration of ambient $PM_{2.5}$ (particles with a diameter < 2.5 µm), whereas the H_2O_2 yields exhibited no clear trend. The abundances of water-soluble transition metals and aromatics in ambient $PM_{2.5}$ were positively correlated with the relative fraction of $^{\bullet}OH$ to the totally detected radicals, but negatively correlated with the relative fraction of carbon-centered radicals. Moreover, we found that the relative fractions of different types of radicals formed by ambient $PM_{2.5}$ were comparable to the surrogate mixtures comprising transition metals, organic hydroperoxide, H_2O_2, and humic or fulvic acids. Therein humic and fulvic acids exhibited strong radical scavenging effect to substantially decrease the radical yield of mixtures comprising cumene hydroperoxide and Fe^{2+}. The interplay of transition metals (e.g., iron), highly oxidized compounds (e.g., organic hydroperoxides), and complexing agents (e.g., humic or fulvic acids), leads to non-linear concentration dependencies of production and yields of different types of RS. Our findings show that how the composition of $PM_{2.5}$ influences the amount and nature of RS produced upon interaction with water, which may explain differences in the chemical reactivity and health effects of particulate matter in clean and polluted air.

https://doi.org/10.5194/acp-2020-973
Preprint. Discussion started: 20 October 2020

Atmospheric Chemistry and Physics Discussions

1 Introduction

Atmospheric fine particulate matter with a particle diameter < 2.5 µm ($PM_{2.5}$) forms reactive species (RS) upon interaction with water and respiratory antioxidants (Bates et al., 2015;Lakey et al., 2016;Park et al., 2018;Li et al., 2018;Tong et al., 2019). The umbrella term RS comprises reactive oxygen species (e.g., $^{\bullet}OH$, $O_2^{\bullet-}$, $^1O_2$, H_2O_2, and ROOH) as well as C- and O-centered organic radicals (Halliwell and Whiteman, 2004;Sies et al., 2017), which influence the chemical aging of atmospheric aerosols and their interaction with the biosphere (Pöschl and Shiraiwa, 2015;Reinmuth-Selzle et al., 2017;Shiraiwa et al., 2017). For example, Fenton-like reactions of hydroperoxides with transition metal ions contribute to the formation of aqueous-phase radicals including $^{\bullet}OH$ (Jacob, 2000;Enami et al., 2014;Anglada et al., 2015;Tong et al., 2016a), enhancing the conversion of organic precursors to secondary organic aerosols (SOA) (Donaldson and Valsaraj, 2010;Ervens et al., 2011;Gligorovski et al., 2015;Gilardoni et al., 2016). Moreover, $PM_{2.5}$ may generate excess concentrations of RS in human airways, causing antioxidant depletion, oxidative stress, and respiratory diseases (Nel, 2005;Cui et al., 2015;Lakey et al., 2016;Qu et al., 2017;Lelieveld and Pöschl, 2017;Rao et al., 2018).

The formation pathways and yields of RS from ambient PM and laboratory-generated SOA have been investigated in a wide range of studies (Valavanidis et al., 2005;Ohyama et al., 2007;Chen et al., 2010;Wang et al., 2011a;Wang et al., 2011b;Verma et al., 2014;Badali et al., 2015;Bates et al., 2015;Verma et al., 2015;Arangio et al., 2016;Tong et al., 2016a;Kuang et al., 2017;Tong et al., 2017;Zhou et al., 2018;Tong et al., 2019;Chowdhury et al., 2019;Fang et al., 2019;Liu et al., 2020). The mass, surface area, and chemical composition of PM were discussed as key factors influencing the reactivity of atmospheric aerosols (Møller et al., 2010;Fang et al., 2015;Jin et al., 2019). Among the substance groups associated with RS formation by PM in water are black carbon (Baumgartner et al., 2014), transition metals (Yu et al., 2018), oxidized aromatic compounds including quinones and environmentally persistent free radicals (Xia et al., 2004;Gehling et al., 2014;Charrier et al., 2014;Xiong et al., 2017), humic-like substances (Lin and Yu, 2011;Page et al., 2012;Fang et al., 2019), and peroxide-containing highly oxygenated organic molecules

https://doi.org/10.5194/acp-2020-973
Preprint. Discussion started: 20 October 2020


Atmospheric Chemistry and Physics Discussions

(HOMs) (Chen et al., 2010;Wang et al., 2011b;Tong et al., 2016a;Tong et al., 2018;Tong et al., 2019;Fang et al., 2020;Qiu et al., 2020). Moreover, the humic-like substances and other multifunctional compounds containing carboxyl, carboxylate, phenolic, and quinoid groups may influence the redox activity of PM via chelating transition metals (Laglera and van den Berg, 2009;Kostić et al., 2011;Catrouillet et al., 2014;Gonzalez et al., 2017;Wang et al., 2018c;Win et al., 2018;Wei et al., 2019).

To assess the oxidative potential of ambient PM, the following cellular or acellular assays have been used: dichloro-dihydro-fluorescein diacetate (DCFH-DA), dithiothreitol (DTT), ascorbic acid (AA), macrophage, electron paramagnetic resonance (EPR), and surrogate lung fluids (SLF) (Landreman et al., 2008;Charrier and Anastasio, 2012;Kalyanaraman et al., 2012;Charrier et al., 2014;Charrier and Anastasio, 2015;Fang et al., 2016;Tong et al., 2018;Bates et al., 2019;Fang et al., 2019;Molina et al., 2020;Crobeddu et al., 2020). However, the interplay of different PM constituents often results in non-additive characteristics of the RS yields or oxidative potential of PM (Charrier et al., 2014;Lakey et al., 2016;Wang et al., 2018b). Thus, unraveling the adverse health effects of ambient PM requires systematic investigations of the RS formation and chemical reactivity of PM from different sources and environments (Shiraiwa et al., 2017).

The concentration of $PM_{2.5}$ and the composition of airborne organic matter vary considerably from clean forest to polluted urban environments. For example, the $PM_{2.5}$ concentrations at the Hyytiälä forest site are typically below 10 μg m^{-3}, with organic matter accounting for ~70% (Laakso et al., 2003;Maenhaut et al., 2011), whereas the $PM_{2.5}$ concentrations in Beijing during winter can reach and exceed daily average values of 150 μg m^{-3}, with organic matter accounting for ~40% (Huang et al., 2014). Moreover, anthropogenic emissions can enhance the formation of biogenic SOA and HOM as well as the levels of particulate transition metals, humic-like substances, and PM oxidative potential (Goldstein et al., 2009;Hoyle et al., 2011;Liu et al., 2014;Xu et al., 2015;Ma et al., 2018;Pye et al., 2019;Shrivastava et al., 2019).

In this study, we compared the RS yields of $PM_{2.5}$ in clean and polluted environments. We used three approaches to explore the RS formation by $PM_{2.5}$ from remote forest of Hyytiälä (Finland), intermediately polluted city of Mainz (Germany), and heavily polluted megacity of Beijing (China) (Figure 1). To quantify

https://doi.org/10.5194/acp-2020-973
Preprint. Discussion started: 20 October 2020

Atmospheric Chemistry and Physics Discussions

the abundances of redox-active PM constituents related to RS formation, we collected ambient $PM_{2.5}$ and measured the chemical composition of organic matter, the abundance of water-soluble transition metals, and the yield of radicals and H_2O_2 in the liquid phase (Figure 1a). To assess the influence of anthropogenic-biogenic organic matter interactions on the RS formation by ambient $PM_{2.5}$, we analyzed the radical yield of SOA generated by oxidation of mixed anthropogenic and biogenic precursors in a laboratory chamber (Figure 1b). To get insights into the radical formation mechanism of ambient $PM_{2.5}$ in water, we differentiated the influence of transition metals, organic hydroperoxide (ROOH), water-soluble humic acid (HA) and fulvic acid (FA) on the radical formation by Fenton-like reactions (Figure 1c).

2 Materials and methods

2.1 Chemicals

The following chemicals were used as received without further purification: β-pinene (99%, Sigma-Aldrich), naphthalene (99.6%, Alfa Aesar GmbH&Co KG), cumene hydroperoxide (80%, Sigma-Aldrich), H_2O_2 (30%, Sigma-Aldrich), $FeSO_4$•$7H_2O$ (F7002, Sigma-Aldrich), $CuSO_4$•$5H_2O$ (209198, Sigma-Aldrich), $NiCl_2$ (98%, Sigma-Aldrich), $MnCl_2$ (≥99%, Sigma-Aldrich), VCl_2 (85%, Sigma-Aldrich), NaCl (443824T, VWR International GmbH), KH_2PO_4 (≥99%, Alfa Aesar GmbH&Co KG), Na_2HPO_4 (≥99.999%, Fluka), humic acid (53680, Sigma-Aldrich), fulvic acid (AG-CN2-0135-M005, Adipogen), 5-tert-Butoxycarbonyl-5-methyl-1-pyrroline-N-oxide (BMPO, high purity, Enzo Life Sciences, Inc.), H_2O_2 assay kit (MAK165, Sigma-Aldrich), ultra-pure water (14211-1L-F, Sigma-Aldrich), 47 mm diameter Teflon filters (JVWP04700, Omnipore membrane filter), and micropipettes (50 µL, Brand GmbH&Co KG). The used neutral saline (pH=7.4) consists of 10 mM phosphate buffer (2.2 mM KH_2PO_4 and 7.8 mM Na_2HPO_4) and 114 mM NaCl, which was used to simulate physiologically relevant condition.

2.2 Collection and extraction of ambient fine PM

Ambient fine particles were collected onto Teflon filters for all sites. The Hyytiälä $PM_{2.5}$ was collected using a three-stage cascade impactor (Dekati® PM10) at the Station for Measuring Forest Ecosystem-Atmosphere Relations station (SMEAR II station, Finland) during 31 May-19 July 2017 (Hari and Kulmala,

https://doi.org/10.5194/acp-2020-973
Preprint. Discussion started: 20 October 2020

Atmospheric Chemistry and Physics Discussions

2005). The Mainz fine PM was collected using a micro-orifice uniform deposit impactor (MOUDI, 122-R, MSP Corporation) (Arangio et al., 2016) on the roof of Max Planck Institute for Chemistry during 22 August-17 November 2017 and 23-31 August 2018. The Beijing winter $PM_{2.5}$ was collected using a 4-channel $PM_{2.5}$ air sampler (TH-16, Wuhan Tianhong Instruments Co., Ltd.) in the campus of the Peking University, an urban site of Beijing, during 20 December-13 January 2016 and 6 November-17 January 2018 (Lin et al., 2015). The sampling time for a single filter sample in Hyytiälä, Mainz, and Beijing are 48-72, 25-54, and 5-24 h, respectively, depending on the local PM concentrations. More information about the sampling sites and instrumentation is shown in Table S1. After sampling, all filter samples were put in petri dishes and stored in a -80 ºC freezer before analysis. To determine the mass of collected PM, each filter was weighed before and after the collection using a high sensitivity balance (±10 µg, Mettler Toledo XSE105DU). In Hyytiälä, the PM_1 and $PM_{1\text{-}2.5}$ were separately sampled, which were combined and extracted together to represent $PM_{2.5}$ samples. Mainz PM with cut-size range of 0.056-1.8 µm is taken as a proxy for $PM_{2.5}$. Particle concentrations in aqueous extracts were estimated to be in the range of 200-6000 µg mL^{-1} (Figure S1).

2.3 Formation, collection, and extraction of laboratory-generated SOA

To generate SOA from mixed anthropogenic and biogenic precursors, different concentrations of gas-phase naphthalene and β-pinene were mixed and oxidized in a potential aerosol mass (PAM) chamber, i.e., an oxidation flow reactor (OFR) (Kang et al., 2007;Tong et al., 2018). Naphthalene and β-pinene were used as representative SOA precursors in Beijing and Hyytiälä, respectively (Hakola et al., 2012;Huang et al., 2019). The concentrations of gas-phase O_3 and $^{\bullet}OH$ in the PAM chamber were ~1 ppm and ~5.0×10^{11} cm^{-3}, respectively. SOA was produced by adjusting the relative concentrations of naphthalene to the sum of it with β-pinene (i.e., [naphthalene]/([naphthalene] + [β-pinene])) to be ~9%, ~23%, and ~38%, respectively. The concentrations of naphthalene and β-pinene were 0.2-0.6 ppm and 1.0-2.5 ppm, respectively, which were determined on the basis of a calibration function measured by gas chromatography mass spectrometry (Tong et al., 2018). To investigate the influece of ozone/β-pinene ratios on redox property of SOA, we

https://doi.org/10.5194/acp-2020-973
Preprint. Discussion started: 20 October 2020


Atmospheric Chemistry and Physics Discussions

measured the aqueous phase radical yields of SOA particles formed from oxidation of ~1 ppm and ~2.5 ppm β-pinene with the same concentration of ozone. With a similar purpose, we measured the radial yields of SOA formed from oxidation of ~0.2 ppm and ~0.6 ppm naphthalene by the same concenteation of gas-phase OH radical. The mean radical yields of β-pinene and naphthalene SOA formed at different concentrations of precursors are compared in Sect. 3.4. The number and size distributions of SOA particles were meaured using a scanning mobility particle sizer (SMPS, GRIMM Aerosol Technik GmbH&Co. KG). When the SOA concentration is stable, 47 mm diameter Teflon filters (JVWP04700, Omnipore membrane filter) were used to collect SOA particles, which were extracted into water solutions within 2 minutes after the sampling. More information about the SOA formation, characterization, collection, and extraction can be found in previous studies (Tong et al., 2016a;Tong et al., 2017;Tong et al., 2018;Tong et al., 2019).

2.4 Surrogate mixtures

Considering that cumene hydroperoxide (CHP), humic acid (HA), and fulvic acid (FA) have been used as model compounds mimicking the redox-active substances in biogenic and anthropogenic PM (Lin and Yu, 2011;Ma et al., 2018;Tong et al., 2019), we measured the relative fractions (RF) of different radicals formed by surrogate mixtures of CHP+Fe^{2+}+Cu^{2+}+HA+H_2O_2 to simulate the radical formation by fine PM from Hyytiälä, Mainz, and Beijing. The H_2O_2 was treated as a redox-active constituent preexisting in PM samples before extraction. The following method was used to make HA or FA solutions. First, 0-1000 μg mL^{-1} HA or FA water suspensions were made. Then, the suspensions were sonicated for 3 minutes to accelerate the dissolution of HA or FA. Afterwards, the sonicated suspensions were centrifuged at 6000 rpm (MiniStar, VWR International bvba) for 2 minutes. Finally, the supernatants were taken out from the centrifuge tubes with pipettes and stored in glass vials under 4-8 °C condition before analysis. The HA or FA solutions were prepared freshly day-to-day. To determine the concentrations of dissolved HA or FA, aliquots of the supernatants were dried with pure N_2 flow (1-2 bar) and weighted with a high sensitivity balance (± 0.01 mg, Mettler Toledo XSE105DU). The concentrations of Fe^{2+}, Cu^{2+}, HA, and H_2O_2 in the surrogate mixtures are 43 μM, 3 μM, 4 mg L^{-1}, and 7 μM, which are based on the measurement of ambient PM extracts (Fe^{2+} and Cu^{2+}, Section 2.8) or the estimated abundance in ambient PM (CHP, HA, FA, and H_2O_2, SI). To explore

https://doi.org/10.5194/acp-2020-973
Preprint. Discussion started: 20 October 2020

Atmospheric Chemistry and Physics Discussions

the influence of HA/FA on Fenton-like reactions, the radical formation in the following aqueous mixtures was also analyzed: CHP+Fe^{2+}, CHP+Cu^{2+}, CHP+Cu^{2+}+HA, CHP+Cu^{2+}+FA. The concentrations of Fe^{2+}, Cu^{2+}, HA, FA, and H_2O_2 in these solutions are 15-300 µM, 15-300 µM, 0-180 µg mL^{-1}, 0-180 µg mL^{-1}, 0-300 µM, respectively.

2.5 Quantification of radicals by EPR

5-tert-Butoxycarbonyl-5-methyl-1-pyrroline-N-oxide (BMPO) was used as a spin-trapping agent for detecting different types of radicals formed in the extracts of PM. Ambient PM or laboratory-generated SOA were extracted from Teflon filters into 10 mM BMPO neutral saline or water solutions by vortex shaking for ~15 minutes (with Heidolph Reax 1). Around one fourth of each ambient PM filter or a whole SOA-loaded filter was used for extraction. It was assumed that during the extraction process, most of the short-lived radicals have reacted with BMPO to form stable adducts.

A continuous-wave electron paramagnetic resonance (CW-EPR) X-band spectrometer (EMXplus-10/12; Bruker Corporation) was applied for the identification and quantification of radical adducts (Tong et al., 2016a;Tong et al., 2017;Tong et al., 2018;Tong et al., 2019). In order to increase the signal to noise ratio of EPR spectra, some of the extracts were concentrated by a factor of 5 - 20 through 15 - 20 minutes drying under 1-2 bar pure N_2 flow. The EPR spectra of BMPO-radical adducts were recorded by setting the following operating parameters: a microwave frequency of 9.84 GHz, a microwave power of 0.017 mW (20 dB), a receiver gain of 40 dB, a modulation amplitude of 1 G, a scan number of 50, a sweep width of 100 G, a modulation frequency of 100 kHz, a conversion time of 11 ms, and a time constant of 10 ms.

To average EPR spectra of different $PM_{2.5}$ extracts for each site, the magnetic field values of each spectrum was transformed to g-values. Then we used the Bruker software, Xenon to do the averaging, irrespective of the concentrations of $PM_{2.5}$ in extracts. The spin-counting method embedded in Xenon was applied to quantify radical adducts. The spin-counting method was calibrated using the standard compound 4-hydroxy-2,2,6,6-tetramethylpiperidin-1-oxyl (TEMPOL). To obtain the relative yields of $^{\bullet}OH$, $O_2^{\bullet-}$, C- and O-centered organic radicals, EPR spectra were simulated and fitted using the Xenon software before

https://doi.org/10.5194/acp-2020-973
Preprint. Discussion started: 20 October 2020

Atmospheric Chemistry and Physics Discussions

deconvolution (Arangio et al., 2016;Tong et al., 2018). The weight of assigned species accounts on average for more than 95% of totally observed radical adducts, which is characterized by the peak area ratios of corresponding species. EPR spectra with low signal-to-noise ratio introduce uncertainty into the parameters describing the lineshape of peaks representing radical adducts (Tseitlin et al., 2012), causing a total quantification uncertainty of 0-19% for the weight and total concentrations of different radical species. The hyperfine coupling constants used for spectrum fitting are shown in Table S2. More information on the hyperfine coupling constants of different types of BMPO radical adducts can be found in previous studies (Zhao et al., 2001;Arangio et al., 2016).

2.6 Measurement of H_2O_2 yields

We extracted ambient $PM_{2.5}$ from one fourth of each Teflon filter into 1 mL ultra-pure water or neutral saline by stirring it with a vortex shaker for ~15 minutes. Afterwards, the extracts were centrifuged at 9000 rpm (Eppendorf Minispin) for 3 minutes to remove the insoluble particles. Finally, the concentration of H_2O_2 in the supernatant was measured using the MAK165 assay kit (Yan et al., 2017;Tong et al., 2018). 50 µL of supernatant and 50 µL of a Master Mix solution containing horseradish peroxidase and Amplex Red substrate were mixed in a 96-well plate. The horseradish peroxidase catalyzed the oxidation of Amplex Red by H_2O_2 to form fluorescent resorufin (Wang et al., 2017), which was consequently quantified using a microplate reader (Synergy™ NEO, BioTek, excitation at 540 nm and emission at 590 nm) after 30 minutes of incubation. The concentration of H_2O_2 in aqueous PM extracts was determined using an H_2O_2 calibration curve based on standard H_2O_2 solutions and also corrected by blank measurements (Tong et al., 2018).

2.7 Mass spectrometry of organic compounds

By using a Q-Exactive Orbitrap mass spectrometer (Thermo Fisher Scientific, MA, USA) coupled with an ultra-high performance liquid chromatography (UHPLC) system (Dionex UltiMate 3000, Thermo Scientific, Germany) (Wang et al., 2018a;Wang et al., 2019;Tong et al., 2019), we characterized the HOMs and aromatic compounds in Hyytiälä, Mainz, and Beijing winter fine PM samples in negative ionization mode. We processed the MS spectrum and UHPLC chromatogram of measured samples through a non-

https://doi.org/10.5194/acp-2020-973
Preprint. Discussion started: 20 October 2020


Atmospheric Chemistry and Physics Discussions

target screening approach by using the commercially available software SIEVE® (Thermo Fisher Scientific, MA, USA). Then, we blank-corrected the signals with peak intensity > 1×10^5. Afterwards, we used the following criteria to assign molecular formulae and filter out the irrational ones: (a) the number of atoms of C, H, O, N, S, and Cl should be in the range of 1-39, 1-72, 0-20, 0-7, 0-4, and 0-2. (b) Atomic ratios of H/C, O/C, N/C, S/C, and Cl/C should be in the range of 0.3-3, 0-3, 0-1.3, 0-0.8, and 0-0.8, respectively.

The HOMs are defined as formulae fell into the following chemical composition range of $C_xH_yO_z$: monomers with x = 8–10, y = 12–16, z = 6–12, and z/x > 0.7; dimers with x = 17–20, y = 26–32 and z = 8–18 (Ehn et al., 2014;Tröstl et al., 2016;Tong et al., 2019). Aromatics in this study are defined to be compounds with aromaticity index (AI) > 0.5 and aromaticity equivalent (X_c) > 2.5, with the parameters accounting for the fraction of oxygen and sulfur atoms involved in π-bond structures of a compound to be set as 1 (Koch and Dittmar, 2006;Yassine et al., 2014;Tong et al., 2016b). Beyond this, The relative abundance of HOMs or aromatic compounds is defined to be the sum chromatographic area of HOMs or aromatics divided by the sum chromatographic area of all assigned organic compounds, with < 30% of totally detected organic compounds not assigned (Wang et al., 2018a).

2.8 Determination of water-soluble transition metal concentrations

Based on the same extraction method as the H_2O_2 analysis in section 2.6, the concentration of five selected water-soluble transition metal species (Fe, Cu, Mn, Ni and V) in the supernatants of $PM_{2.5}$ extracts was quantified using an inductively coupled plasma mass spectrometer (ICP-MS, Agilent 7900). These five transition metal species were chosen for analysis due to their prominent concentrations and higher oxidative potential (Charrier and Anastasio, 2012). A calibration curve for the ICP-MS analysis was made by measuring standard multi-element stock solutions (Custom Grade, Inorganic Ventures). An aliquot of the supernatants was diluted and acidified using a mixture of nitric acid (5%) and hydrofluoric acid (1%), which was finalized to be 5 mL before analysis. The measured transition metal concentrations were blank-corrected and shown in corresponding figures. The detection limit of the ICP-MS analysis in this study was typically < 40 ng L^{-1}. The $PM_{2.5}$ samples collected on 2 June, 7 June, 9 June, 12 June in 2017 in Hyytiälä, on 22 August, 26 August, 28 August, 25 September, 25 October, 14 November in 2017 in Mainz, and all

https://doi.org/10.5194/acp-2020-973
Preprint. Discussion started: 20 October 2020


Atmospheric Chemistry and Physics Discussions

the 12 $PM_{2.5}$ samples from Beijing winter were used for transition metal analysis. Temporal evolution of water-soluble transition metal concentrations in water extracts of Mainz $PM_{2.5}$ were also measured, and we found that the total ion concentration of Fe, Cu, Mn, Ni, and V showed a rapid rise during the first 15 min (Figure S2a), but at a much slower rate afterwards (Figure S2b).

3 Results and discussion

3.1 Relative yields of different types of radicals from ambient $PM_{2.5}$

Figure 2a shows the averaged EPR spectra of BMPO-radical adducts in neutral saline extracts of $PM_{2.5}$ samples from Hyytiälä, Mainz (cut-size range 0.056-1.8 μm PM as a proxy), and Beijing. Each spectrum is composed of multiple peaks attributable to different types of BMPO-radical adducts. The dotted vertical lines with different colors indicate the peaks attributable to adducts of BMPO with •OH (green), $O_2^{\bullet-}$ (orange), C- (blue) and O-centered organic radicals (purple) (Zhao et al., 2001;Arangio et al., 2016), respectively. The spectrum of Hyytiälä $PM_{2.5}$ is dominated by peaks attributable to C-centered radicals. In contrast, the spectrum of Mainz $PM_{2.5}$ comprises strong peaks attributable to •OH and C-centered radicals, with •OH exhibiting stronger signals. Finally, the spectrum of Beijing winter $PM_{2.5}$ is mainly composed of four peaks attributable to •OH.

Figure 2b shows the averaged relative fractions (RF) of •OH, $O_2^{\bullet-}$, C- and O-centered organic radicals generated by multiple PM samples from each site. In line with visual inspection of the spectra in Figure 2a, the $PM_{2.5}$ from clean forest site generates relatively more C- and O-centered organic radicals but less •OH, vice versa for the radical yield by $PM_{2.5}$ from polluted areas. Specifically, the mean RF of C- and O-centered organic radicals, ordered from highest to lowest are: Hyytiälä (66% and 11%) > Mainz (46% and 10%) > Beijing (39% and 5%). Note that, the significantly higher RF of C-centered radicals than O-centered organic radicals may be induced by the higher yield and stability of BMPO-C-centered radical adduct in the liquid phase (De Araujo et al., 2006). Moreover, the C- and O-centered organic radicals may comprise a series of radicals with different molecular structures, the yields of which are associated with aqueous redox chemistry of organic matter such as Fenton-like reactions (Arangio et al., 2016;Tong et al., 2018;Tong et

https://doi.org/10.5194/acp-2020-973
Preprint. Discussion started: 20 October 2020


Atmospheric Chemistry and Physics Discussions

al., 2019). The mean RF of •OH, ordered from lowest to highest are: 21% (Hyytiälä) < 38% (Mainz) < 53% (Beijing). The presence of •OH is related to multiple formation pathways, such as Fenton-like reactions, thermal or hydrolytic decomposition of peroxide-containing HOMs, and redox chemistry of environmentally persistent free radicals or aromatic compounds-containing humic-like substances (Chevallier et al., 2004;Valavanidis et al., 2005;Li et al., 2008;Page et al., 2012;Gehling et al., 2014;Tong et al., 2016a;Tong et al., 2017;Tong et al., 2018;Tong et al., 2019;Qiu et al., 2020). The mean RF of $O_2^{\bullet-}$ only varies slightly in the range of 2-6%, showing no clear trend and within the range of standard errors in Figure 2b.

3.2 Mass-specific and air sample volume-specific yields of RS from ambient $PM_{2.5}$

Figure 3 shows the mass-specific and air sample volume-specific yields of reactive species (RS) including radicals, H_2O_2, and the sum of radicals and H_2O_2 by $PM_{2.5}$ from Hyytiälä, Mainz, and Beijing. The mass-specific yields of RS are shown in the unit of pmol μg^{-1} of $PM_{2.5}$, reflecting the redox activities of $PM_{2.5}$ irrespective of filter loadings. The air sample volume-specific yields of RS are shown in the unit of pmol m^{-3} of air, indicating that the redox activities of $PM_{2.5}$ scale with atmospheric concentration of $PM_{2.5}$. We note that, while the more polluted sampling sites led to higher mass loadings, the concentrations of PM in extracts were found to have a tiny impact on the radical yields (Figure S1c and S1d).

Figure 3a shows that the mass-specific radical yields are negatively correlated with $PM_{2.5}$ mass concentrations. The mean concentrations of $PM_{2.5}$ are lower to higher in the order of 5 (Hyytiälä) < 16 (Mainz) < 202 $\mu g\ m^{-3}$ (Beijing), whereas the radical yields are in a reverse order of 0.58 > 0.33 > 0.07 pmol μg^{-1}. The higher mass-specific radical yield of $PM_{2.5}$ from Hyytiälä may be associated with the higher abundance of particulate organic matter, which includes quinones and organic hydroperoxides that undergo thermal, photonic, or hydrolytical dissociation as well as redox chemistry such as Fenton-like reactions to produce radicals (Badali et al., 2015;Tong et al., 2016a;Tong et al., 2019). More than 70% of $PM_{2.5}$ in Hyytiälä forest is composed of organic matter (Jimenez et al., 2009;Maenhaut et al., 2011), whereas the abundances of organic matter in Mainz autumn and Beijing winter $PM_{2.5}$ are ~40% (Jimenez et al.,

https://doi.org/10.5194/acp-2020-973
Preprint. Discussion started: 20 October 2020


Atmospheric Chemistry and Physics Discussions

2009;Huang et al., 2014), which might in part explain the lower radical yield of these samples. Figure 3a also shows that the mass-specific H_2O_2 yields of $PM_{2.5}$ from Hyytiälä (~2.2 pmol μg^{-1}), Mainz (~3.4 pmol μg^{-1}), and Beijing (~3.4 pmol μg^{-1}) exhibit a weak positive correlation with $PM_{2.5}$ mass concentrations, agreeing with previous measurements of the H_2O_2 formation by fine PM from different districts of Los Angeles (Arellanes et al., 2006;Wang et al., 2012) (Figure S4a). The higher H_2O_2 yield of urban fine PM may be associated with its higher abundance of transition metals and aromatic-containing organic matter (e.g., quinones and humic-like substances), which have been found as redox-active constituents to produce H_2O_2 upon dissolution of ambient PM or laboratory-generated SOA in water (Arellanes et al., 2006;Chung et al., 2006;Wang et al., 2010;Wang et al., 2012). The weak correlation of mass-specific H_2O_2 yields and $PM_{2.5}$ concentrations reflects the varying redox activity of $PM_{2.5}$ from different regions, which is driven by the PM source-dependent composition, abundance, and chemistry of redox active substances (e.g., transition metals and organic matter).

Figures 3b and S4b show that the air sample volume-specific yields of total RS (H_2O_2+radicals) increase as $PM_{2.5}$ concentrations increase, reflecting a higher RS formation in per cubic meter of polluted urban air. Specifically, the relative air sample volume-specific yields of H_2O_2 (i.e., $[H_2O_2]/([H_2O_2]+[radicals])$), ordered from lowest to highest are: 78% (Hyytiälä) > 91% (Mainz) > 97% (Beijing), whereas the relative air sample volume-specific radical yields (i.e., $[radicals]/([H_2O_2]+[radicals])$) are in the reverse order of 22% > 9% > 3%. The relatively stable H_2O_2 becomes increasingly important for the reactivity of ambient $PM_{2.5}$ compared to the more reactive radicals when transitioning from clean to polluted conditions. Due to its stability, H_2O_2 has been found previously to dominate the concentrations of RS formed by $PM_{2.5}$ in liquid phase with the presence of antioxidants but absence of spin traps (Lakey et al., 2016;Tong et al., 2018). This study shows a time integral concentration rather than the RS concentration taking into account the different lifetimes and evolution pathways of radicals and H_2O_2. H_2O_2 still constitutes the biggest fraction of RS detected. Of note, the EPR method may not detect all radicals produced but rather a fraction that is trapped with BMPO before undergoing other radical termination reactions. It is also notable that we measured the RS yields of PM from three different areas. Further measurements of PM from more locations

https://doi.org/10.5194/acp-2020-973
Preprint. Discussion started: 20 October 2020


Atmospheric Chemistry and Physics Discussions

may shift the trend of the RS yields in Figure 3 by a certain degree, the extent of which warranty follow-up studies.

3.3 Correlation of radical yield with chemical composition of ambient $PM_{2.5}$

Figure 4 shows how the relative fractions (RF) of C-centered radicals and $^{\bullet}OH$ in aqueous extracts of ambient $PM_{2.5}$ are correlated with the abundance of HOMs, aromatic compounds, and water-soluble transition metals. Figure 4a shows that the relative abundance of HOMs exhibits a positive correlation with the RF of C-centered radicals, whereas a negative correlation with the RF of $^{\bullet}OH$. The relative abundance of HOMs, ordered from lowest to highest are: ~0.2% (Beijing) < ~6% (Mainz) < ~10% (Hyytiälä) (Tong et al., 2019), and the RF of C-centered radicals is in the same order of 39% < 46% < 66%, but the RF of $^{\bullet}OH$ are in the reverse order of 53% > 38% > 21%. The higher RF of C-centered radicals formed by $PM_{2.5}$ from less-polluted air is in the same trend as the total mass-specific radical yield of $PM_{2.5}$ from these sites (Figure 3a), confirming previous results that peroxide-containing HOMs may play an important role in organic radical formation (Tong et al., 2016a;Tong et al., 2019).

In contrast to HOMs, the relative abundance of aromatic compounds in $PM_{2.5}$ is higher in polluted urban air compared to clean forest: ~0.2% (Hyytiälä) < ~2% (Mainz) < ~16% (Beijing) (Figure 4b), causing a positive correlation with the RF of $^{\bullet}OH$, but a negative correlation with the RF of C-centered radicals. The higher relative abundance of particulate aromatics in Beijing compared to Hyytiälä can be attributed to the stronger anthropogenic emissions (e.g., from traffic) at the polluted urban site (Jimenez et al., 2009;Zhang and Tao, 2009;Elser et al., 2016;An et al., 2019). The chemistry of oxygenated aromatic-containing substances, such as quinones and semiquinones, may enhance the conversion of other RS (e.g., $O_2^{\bullet-}$) into $^{\bullet}OH$ due to redox cycling and interaction with water (Chung et al., 2006;Khachatryan et al., 2011;Fan et al., 2016).

Similar to the aromatics, the transition metal abundances exhibit a positive correlation with the RF of $^{\bullet}OH$, but a negative correlation with the RF of C-centered radicals (Figure 4c). The abundance of water-soluble transition metals in $PM_{2.5}$ from different locations, ordered from lowest to highest are: 13.4

https://doi.org/10.5194/acp-2020-973
Preprint. Discussion started: 20 October 2020

Atmospheric Chemistry and Physics Discussions

(Hyytiälä) < 19.6 (Mainz) < 27.8 (Beijing) pmol μg^{-1}, and the RF of •OH is in the same order of 21% < 38% < 53%, whereas the relative fraction of C-centered radicals is in the reverse order of 66% > 46% > 39%. The consistently higher abundance of water-soluble transition metals and RF of •OH of urban $PM_{2.5}$ may reflect the importance of Fenton-like reactions in radical formation in polluted air, as H_2O_2 and hydroperoxides can be efficiently converted into •OH. Moreover, several studies have reported that metal-organic interactions may alter the oxidative potential and RS yield of PM under atmospheric and physiological conditions (Zuo and Hoigne, 1992;Singh and Gupta, 2016;Cheng et al., 2017;Wang et al., 2018b;Wei et al., 2019;Lin and Yu, 2020). Thus, investigations on the radical chemistry of transition metals strongly benefit from determination of organic aerosols to illuminate the mechanism of RS formation. Finally, additional measurements of $PM_{2.5}$ from more locations may shift the correlation of radical yields and abundances of transition metals and organic matter by a certain degree, the extent of which also warranty follow-up studies.

3.4 Radical yield of laboratory-generated SOA

To investigate the influence of biogenic-anthropogenic organic matter interaction on the formation of aqueous radicals, we measured the radical yield of SOA generated from oxidation of mixed naphthalene and β-pinene precursors. Figure 5a shows that the mass-specific radical yields of SOA decrease with increasing relative concentrations of naphthalene (i.e., [naphthalene]/([naphthalene]+[β-pinene])). As the relative concentration of naphthalene is increased from 0 to 9, 23, and 38%, the radical yields of SOA decrease in the order of ~8.4 > ~3.0 > ~2.3 > ~1.9 pmol μg^{-1}. This is because the naphthalene SOA has a lower radical yield than β-pinene SOA with the same mass concentration in water extracts (Tong et al., 2016a;Tong et al., 2017;Tong et al., 2018;Tong et al., 2019). Moreover, the mass-specific radical yield of β-pinene SOA in Figure 5a is the mean value of SOA from ~1 ppm and ~2.5 ppm of β-pinene (see Sect. 2.3). Therein the SOA from ~2.5 ppm β-pinene exhibits higher radical yield (11.5 pmol μg^{-1}) than the SOA generated from ~1 ppm β-pinene (4.5 pmol μg^{-1}), which may be associated with the increasing partition of oligomers into the particle phase with higher starting concentration of β-pinene (Kourtchev et al., 2016).

https://doi.org/10.5194/acp-2020-973
Preprint. Discussion started: 20 October 2020


Atmospheric Chemistry and Physics Discussions

Some oligomers contain peroxide functional groups accounting for a major fraction of HOMs (Krapf et al., 2016). The radical yield of naphthalene SOA in Figure 5 is the average yields of SOA formed by the oxidation of ~0.2 ppm and ~0.6 ppm naphthalene (see section 2.3), respectively. Therein the radical yield of SOA from ~0.2 ppm naphthalene (1.1 pmol μg^{-1}) is slightly higher than the SOA from ~0.6 ppm naphthalene (0.8 pmol μg^{-1}), agreeing with the finding of enhanced oxidative potential of naphthalene SOA formed under higher oxidant/naphthalene ratio condition (Wang et al., 2018b).

Figure 5b shows that β-pinene SOA mainly generates $^{\bullet}OH$ (~86%), whereas the mixed precursor SOA and naphthalene SOA mainly generate $O_2^{\bullet-}$ (60-77%) and C-centered radicals (18-34%), which is in line with our previous findings (Tong et al., 2016a;Tong et al., 2018;Tong et al., 2019). The much lower RF of $^{\bullet}OH$ formed by mixed precursor SOA (< 10%) may mainly be due to its lower abundance of peroxide-containing HOMs. It is notable that $PM_{2.5}$ from polluted Beijing contains substantial amount of aromatics (Figure 4b), but mainly generates $^{\bullet}OH$ upon interaction with water, which seems to contradict our finding that naphthalene SOA generates $^{\bullet}OH$ only to a small extent. This may be related to the more complex composition of the ambient PM compared to laboratory-generated SOA. For example, conversion of $O_2^{\bullet-}$ to $^{\bullet}OH$, H_2O_2, and O_2 by transition metals or other redox-active PM constituents through Haber-Weiss reactions or other related redox chemistry (Kehrer, 2000;Tong et al., 2016a) is expected to occur in ambient samples, but would not be observed in laboratory-generated SOA that does not contain significant fractions of transition metals.

3.5 Radical yield of surrogate mixtures comprising transition metals, CHP, HA, FA and H_2O_2

Figure 6a shows the concentration of radicals formed in aqueous mixtures comprising 0-25 μM cumene hydroperoxide (CHP), 43 μM Fe^{2+}, 3 μM Cu^{2+}, 4 μg mL^{-1} humic acid (HA) and 7 μM H_2O_2, with mixtures containing 0, 5, and 25 μM CHP to be treated as surrogates of redox-active constituents in PM from Beijing, Mainz, and Hyytiälä. As the concentration of CHP is increased from 0 to 25 μM, the total concentration of detectable radicals increases from 0.4 to 2.8 μM, with the relative fractions (RF) of C-centered radicals increase from 1% to 30%, whereas the RF of $^{\bullet}OH$ and O-centered organic radicals decreases from 72% to

https://doi.org/10.5194/acp-2020-973
Preprint. Discussion started: 20 October 2020

Atmospheric Chemistry and Physics Discussions

60% and from ~23% to ~8% (Figure 6b), respectively. The higher RF of C-centered radicals but lower RF of •OH formed at higher concentration of CHP resembles the radical yield of ambient fine PM from cleaner areas (Figure 2b), which contains a large fraction of HOMs (Tong et al., 2019). Moreover, Figure S5 shows that adding 75, 100, 150, 200, and 300 μM H_2O_2 significantly and linearly (R^2=0.95) elevates the •OH concentration in aqueous mixtures comprising CHP, Fe^{2+}, HA, and H_2O_2. Thus, the higher RF of •OH in surrogate mixtures (Figure 6b) compared with ambient PM extracts (Figure 2b) may be due to the choice of a slightly higher concentration of H_2O_2 in the surrogate mixture (7 μM, see SI).

To compare the Fenton-like reactions initiated by different transition metal ions related to ambient $PM_{2.5}$, we measured the absolute and relative racial yields of aqueous mixtures containing CHP and different transition metal species, such as Fe^{2+}, Cu^{2+}, Mn^{2+}, or Ni^{2+}. We found that Fe^{2+} is most efficient in initiating Fenton-like reactions (Deguillaume et al., 2005) and the BMPO-radical adduct concentrations varied along the reaction time (Figure S6). Of note, the abundance, chemical composition, and physicochemical properties of the redox-active constituents in ambient PM (e.g., transition metals and organic matter) can be different from the surrogate mixtures, causing partially different radical yields between surrogate mixtures and ambient $PM_{2.5}$ (e.g., less comparable RF of •OH than the RF of C-centered radicals), which warrants follow-up studies. To simplify the discussion, we only show the radical yields as mean values within ~25 minutes of extraction and measurement.

To assess the influence of humic acid on Fenton-like reactions, we measured the radical yields of mixtures comprising 100 μM CHP, 300 μM Fe^{2+}, and 0-180 μg mL^{-1} HA. As the concentration of HA is increased from 0 to 36 μg mL^{-1}, the concentration of total formed radicals decreased by ~52% from 15.5 to 7.4 μM (Figure 6c). This may be associated with the following properties of HA. First, HA exhibits pronounced iron binding capacity of 32 nmol Fe per milligram of HA, preferentially toward Fe^{3+} rather than Fe^{2+} (Laglera and van den Berg, 2009;Scheinhardt et al., 2013). Thus, HA may interfere in the redox cycling of Fe^{2+} and Fe^{3+} by chelating them. The lower concentration of free iron ions may prevent the formation of radicals via Fenton-like reactions. Second, humic substances have been found to exhibit antioxidant

https://doi.org/10.5194/acp-2020-973
Preprint. Discussion started: 20 October 2020


Atmospheric Chemistry and Physics Discussions

properties (Aeschbacher et al., 2012), thus the HA used for Figure 6c may act as an RS scavenger, therefore terminating radical processes and reducing the overall radical concentration. As the HA concentration is increased further from 36 to 180 μg mL^{-1}, the radical concentration is reduced slightly, by less than 20%. This plateau of radical concentration is accompanied by an increasing RF of C-centered radicals (Figure 6d), indicating that HA may also be involved in more complex radical chemistry with $O_2^{\bullet-}$, $^{\bullet}OH$, or oxygen-centered organic radicals enhancing carbon-centered radical formation (Shi et al., 2020). In fact, the RF of C-centered radicals steeply increases from ~19% to ~94% as the HA concentration is increased from 0 to 180 μg mL^{-1}, whereas the RF of $O_2^{\bullet-}$ and $^{\bullet}OH$ decreases from ~59% and ~21% to ~3%. The higher RF of C-centered radicals but lower RF of $O_2^{\bullet-}$ and $^{\bullet}OH$ at higher concentration of HA may be induced by the reactions of HA with $O_2^{\bullet-}$ and $^{\bullet}OH$. The RF of O-centered organic radicals does not exhibit a consistent trend and varies within the range of 5-20%. Moreover, we found that the reaction between HA and CHP (in the absence of Fe ions) produces only a negligible amount of radicals (not shown), which indicates that HA may mainly influence the radical formation upon interaction with iron ions or radicals formed by Fenton-like reactions, but does not form prominent amount of radicals by reactions with CHP or through the decomposition of CHP at the applied concentrations.

Fulvic acid (FA) is another kind of typical atmospheric humic-like substances exerting metal chelating activity (Graber and Rudich, 2006;Tang et al., 2014). Thus, we also measured the radical yields of the mixtures comprising CHP, transition metals, and FA. As shown in Figure 6e, the concentration of radicals formed by mixtures comprising 100 μM CHP, 300 μM Fe^{2+}, and FA decreases by ~10% as the concentration of FA is increased from 6 to 36 μg mL^{-1}. Therein the $O_2^{\bullet-}$ is the dominant radial species, accounting for > 59% of totally formed radicals (Figure 6f). The $O_2^{\bullet-}$ may be generated via multiple redox reaction pathways such as oxidation of Fe^{2+} or decomposition of organic peroxy radicals (Chevallier et al., 2004). Figure 6f also shows that RF of $^{\bullet}OH$, $O_2^{\bullet-}$, C- and O-centered organic radicals varies slightly, which is different from the decreasing radical yield by Fenton-like reaction system containing HA (Figure 6c), but agreeing with the lower capacity of FA (16.7±2.0 nmol mg^{-1}) than HA (32.0±2.2 nmol mg^{-1}) in binding

https://doi.org/10.5194/acp-2020-973
Preprint. Discussion started: 20 October 2020

Atmospheric Chemistry and Physics Discussions

Fe(III) (Laglera and van den Berg, 2009). As the concentration of FA is increased further to 12 μg mL^{-1}, the observed radical concentration in aqueous mixtures of CHP+Fe^{2+}+FA decreases significantly to ~9.6 μM, which may mainly be associated with the formation of Fe-FA complexes and the radical scavenging effect of FA as discussed for HA above (Wang et al., 1996;Scheinhardt et al., 2013;Yang et al., 2017). During this process, the RF of C-centered radicals increases for 3-fold to be ~28%, indicating that FA may also be oxidized by different types of oxidants to form C-centered radicals (Gonzalez et al., 2017), similar to HA in Figure 6c. As the concentration of FA is increased further to 180 μg mL^{-1}, the concentration of totally formed radicals decreases further to 7.6 μM, the RF of C-centered radicals increases further to ~36%, whereas the RF of •OH and O-centered organic radicals decreases significantly to 4-5% and below the detecting limit, respectively (Figure 6f). Moreover, the Figure S7 indicates that the RF of different radicals formed by mixtures comprising CHP, Cu^{2+} and FA exhibited a different trend from the mixtures of CHP, Fe^{2+}, and FA, indicating that FA might influence the radical formation by Cu^{2+} initiated Fenton-like reactions in a efficiency different from the Fe^{2+} initiated Fenton-like reactions.

4 Conclusions and implications

In this study, we found that $PM_{2.5}$ levels exhibit a negative correlation with the mass-specific radical yields, but a weak positive correlation with the H_2O_2 yields. We also found that the mass-specific concentration of transition metals and relative abundance of aromatic compounds are higher in the urban air than the remote forest, in the order of Hyytiälä < Mainz < Beijing. The relative fractions (RF) of •OH formed by different source $PM_{2.5}$ in water is in the same order as the relative abundances of transition metals and aromatics, indicating that urban fine PM favors the formation of OH radicals upon redox chemistry of transition metals, aromatics, or transition metal-aromatic interactions in water. The relative abundance of highly oxygenated organic molecules (HOMs) exhibits a reverse trend compared to aromatics and transition metals, but is in a positive correlation with the RF of C-centered radicals, confirming the strong association of HOMs with organic radical formation by $PM_{2.5}$ in water (Tong et al., 2019).

https://doi.org/10.5194/acp-2020-973
Preprint. Discussion started: 20 October 2020


Atmospheric Chemistry and Physics Discussions

We also measured the radical yield of laboratory-generated SOA from mixing the biogenic SOA precursor β-pinene and the anthropogenic SOA precursor naphthalene. We found that the relative fractions of naphthalene SOA of the totally formed SOA significantly influence the amount and types of radicals formed by the mixed precursor SOA in water with •OH radicals dominating pure β-pinene SOA, Carbon-centered radicals becoming increasingly dominant as the fraction of naphthalene increases. To get insights into the Fenton-like reactions in aqueous extracts of ambient $PM_{2.5}$, we investigated the radical formation by surrogate mixtures comprising cumene hydroperoxide, transition metals, water-soluble humic acid (HA) or fulvic acid (FA), and H_2O_2. We found that HA and FA exhibit different radical scavenging and antioxidant activity in suppressing the radical formation from Fenton-like reactions.

The synthetic application of ambient $PM_{2.5}$ characterization, chamber simulation, and surrogate mixture measurement in this study provides a novel approach to investigate the RS chemistry of atmospheric particles. The direct analysis of ambient $PM_{2.5}$ enables us to find and quantify the key component (e.g., HOMs, aromatics, or transition metals) of $PM_{2.5}$ that may influence its reactivity. The investigation of laboratory-generated SOA enables us to assess the influence of anthropogenic-biogenic organic component interactions on the radical formation by ambient PM. The measurement of surrogate or aqueous mixtures of model substances (transition metals, CHP, HA, FA, and H_2O_2) enables us to clarify the role of individual redox active compound as well as their interplays in the radical chemistry of PM, including Fenton-like reactions, transition metal-organic interactions, or subsequent chain reactions. Based on this systematic analysis, we quantitatively compared the RS formation mechanism of particulate matter from air ranging from clean to heavily polluted areas. The higher relative amount of detected radicals and H_2O_2 formed by urban $PM_{2.5}$ can be seen as a measure of higher potential oxidative damage caused by air pollutants in the epithelial lining fluid of the human respiratory tract. These newly achieved insights enable a better understanding of the influence of biogenic and anthropogenic emissions on atmospheric chemistry, air quality, and public health in the Anthropocene (Pöschl and Shiraiwa, 2015;Cheng et al., 2016;Shiraiwa et al., 2017). Finally, the composition and concentration of organic molecules have been found to influence its role in transition metal-initiated radical chemistry. For instance, carboxylic acids enhance the oxidative

https://doi.org/10.5194/acp-2020-973
Preprint. Discussion started: 20 October 2020


Atmospheric Chemistry and Physics Discussions

potential of transition metals, whereas the imidazoles suppress it (Lin and Yu, 2020). Moreover, low concentration of oxalate forms mono-complexes with Fe^{2+}, but high concentration of oxalate scavenges OH radicals (Fang et al., 2020). Thus, the role of different humic-like substances component in Fenton-like reactions and its impact on aerosol reactivity have not been fully addressed, which warrants follow up studies.

https://doi.org/10.5194/acp-2020-973
Preprint. Discussion started: 20 October 2020

Atmospheric Chemistry and Physics Discussions

References

Aeschbacher, M., Graf, C., Schwarzenbach, R. P., and Sander, M.: Antioxidant properties of humic substances, Environ. Sci. Technol., 46, 4916-4925, 2012.

An, Z., Huang, R.-J., Zhang, R., Tie, X., Li, G., Cao, J., Zhou, W., Shi, Z., Han, Y., and Gu, Z.: Severe haze in Northern China: A synergy of anthropogenic emissions and atmospheric processes, Proc. Natl. Acad. Sci. U.S.A., 116, 8657-8666, 2019.

Anglada, J. M., Martins-Costa, M., Francisco, J. S., and Ruiz-Lopez, M. F.: Interconnection of reactive oxygen species chemistry across the interfaces of atmospheric, environmental, and biological processes, Acc. Chem. Res., 48, 575-583, 2015.

Arangio, A. M., Tong, H., Socorro, J., Pöschl, U., and Shiraiwa, M.: Quantification of environmentally persistent free radicals and reactive oxygen species in atmospheric aerosol particles, Atmos. Chem. Phys., 16, 13105-13119, 2016.

Arellanes, C., Paulson, S. E., Fine, P. M., and Sioutas, C.: Exceeding of Henry's law by hydrogen peroxide associated with urban aerosols, Environ. Sci. Technol., 40, 4859-4866, 2006.

Badali, K., Zhou, S., Aljawhary, D., Antiñolo, M., Chen, W., Lok, A., Mungall, E., Wong, J., Zhao, R., and Abbatt, J.: Formation of hydroxyl radicals from photolysis of secondary organic aerosol material, Atmos. Chem. Phys., 15, 7831-7840, 2015.

Bates, J. T., Weber, R. J., Abrams, J., Verma, V., Fang, T., Klein, M., Strickland, M. J., Sarnat, S. E., Chang, H. H., and Mulholland, J. A.: Reactive oxygen species generation linked to sources of atmospheric particulate matter and cardiorespiratory effects, Environ. Sci. Technol., 49, 13605-13612, 2015.

Bates, J. T., Fang, T., Verma, V., Zeng, L., Weber, R. J., Tolbert, P. E., Abrams, J. Y., Sarnat, S. E., Klein, M., Mulholland, J. A., and Russell, A. G.: Review of acellular assays of ambient particulate matter oxidative potential: Methods and relationships with composition, sources, and health effects, Environ. Sci. Technol., 53, 4003-4019, 2019.

Baumgartner, J., Zhang, Y., Schauer, J. J., Huang, W., Wang, Y., and Ezzati, M.: Highway proximity and black carbon from cookstoves as a risk factor for higher blood pressure in rural China, Proc. Natl. Acad. Sci. U.S.A., 111, 13229-13234, 2014.

Catrouillet, C., Davranche, M., Dia, A., Bouhnik-Le Coz, M., Marsac, R., Pourret, O., and Gruau, G.: Geochemical modeling of Fe (II) binding to humic and fulvic acids, Chem. Geol., 372, 109-118, 2014.

Charrier, J., and Anastasio, C.: On dithiothreitol (DTT) as a measure of oxidative potential for ambient particles: evidence for the importance of soluble transition metals, Atmos. Chem. Phys., 12, 9321-9333, 2012.

https://doi.org/10.5194/acp-2020-973
Preprint. Discussion started: 20 October 2020

Charrier, J. G., McFall, A. S., Richards-Henderson, N. K., and Anastasio, C.: Hydrogen peroxide formation in a surrogate lung fluid by transition metals and quinones present in particulate matter, Environ. Sci. Technol., 48, 7010-7017, 2014.

Charrier, J. G., and Anastasio, C.: Rates of hydroxyl radical production from transition metals and quinones in a surrogate lung fluid, Environ. Sci. Technol., 49, 9317-9325, 2015.

Chen, X., Hopke, P. K., and Carter, W. P.: Secondary organic aerosol from ozonolysis of biogenic volatile organic compounds: chamber studies of particle and reactive oxygen species formation, Environ. Sci. Technol., 45, 276-282, 2010.

Cheng, C., Li, M., Chan, C. K., Tong, H., Chen, C., Chen, D., Wu, D., Li, L., Wu, C., and Cheng, P.: Mixing state of oxalic acid containing particles in the rural area of Pearl River Delta, China: implications for the formation mechanism of oxalic acid, Atmos. Chem. Phys., 17, 9519-9533, 2017.

Cheng, Y., Zheng, G., Wei, C., Mu, Q., Zheng, B., Wang, Z., Gao, M., Zhang, Q., He, K., and Carmichael, G.: Reactive nitrogen chemistry in aerosol water as a source of sulfate during haze events in China, Sci. Adv., 2, e1601530, 2016.

Chevallier, E., Jolibois, R. D., Meunier, N., Carlier, P., and Monod, A.: "Fenton-like" reactions of methylhydroperoxide and ethylhydroperoxide with Fe^{2+} in liquid aerosols under tropospheric conditions, Atmos. Environ., 38, 921-933, 2004.

Chowdhury, P. H., He, Q., Carmieli, R., Li, C., Rudich, Y., and Pardo, M.: Connecting the Oxidative Potential of Secondary Organic Aerosols with Reactive Oxygen Species in Exposed Lung Cells, Environ. Sci. Technol., 53, 13949-13958, 2019.

Chung, M. Y., Lazaro, R. A., Lim, D., Jackson, J., Lyon, J., Rendulic, D., and Hasson, A. S.: Aerosol-borne quinones and reactive oxygen species generation by particulate matter extracts, Environ. Sci. Technol., 40, 4880-4886, 2006.

Crobeddu, B., Baudrimont, I., Deweirdt, J., Sciare, J., Badel, A., Camproux, A.-C., Bui, L. C., and Baeza-Squiban, A.: Lung Antioxidant Depletion: A Predictive Indicator of Cellular Stress Induced by Ambient Fine Particles, Environ. Sci. Technol., 54, 2360-2369, 2020.

Cui, Y., Xie, X., Jia, F., He, J., Li, Z., Fu, M., Hao, H., Liu, Y., Liu, J. Z., and Cowan, P. J.: Ambient fine particulate matter induces apoptosis of endothelial progenitor cells through reactive oxygen species formation, Cell Physiol. Biochem., 35, 353-363, 2015.

De Araujo, M., De M. Carneiro, J., and Taranto, A.: Solvent effects on the relative stability of radicals derived from artemisinin: DFT study using the PCM/COSMO approach, Int. J. Quantum. Chem., 106, 2804-2810, 2006.

https://doi.org/10.5194/acp-2020-973
Preprint. Discussion started: 20 October 2020


Atmospheric Chemistry and Physics Discussions

572 Deguillaume, L., Leriche, M., Desboeufs, K., Mailhot, G., George, C., and Chaumerliac, N.: Transition
573 metals in atmospheric liquid phases: Sources, reactivity, and sensitive parameters, Chem. Rev., 105, 3388-
574 3431, 2005.
575 Donaldson, D., and Valsaraj, K. T.: Adsorption and reaction of trace gas-phase organic compounds on
576 atmospheric water film surfaces: A critical review, Environ. Sci. Technol., 44, 865-873, 2010.
577 Ehn, M., Thornton, J. A., Kleist, E., Sipilä, M., Junninen, H., Pullinen, I., Springer, M., Rubach, F.,
578 Tillmann, R., and Lee, B.: A large source of low-volatility secondary organic aerosol, Nature, 506, 476-
579 479, 2014.
580 Elser, M., Huang, R.-J., Wolf, R., Slowik, J. G., Wang, Q., Canonaco, F., Li, G., Bozzetti, C., Daellenbach,
581 K. R., and Huang, Y.: New insights into $PM_{2.5}$ chemical composition and sources in two major cities in
582 China during extreme haze events using aerosol mass spectrometry, Atmos. Chem. Phys., 16, 3207-3225,
583 2016.
584 Enami, S., Sakamoto, Y., and Colussi, A. J.: Fenton chemistry at aqueous interfaces, Proc. Natl. Acad. Sci.
585 U.S.A., 111, 623-628, 2014.
586 Ervens, B., Turpin, B., and Weber, R.: Secondary organic aerosol formation in cloud droplets and aqueous
587 particles (aqSOA): a review of laboratory, field and model studies, Atmos. Chem. Phys., 11, 11069-11102,
588 2011.
589 Fan, X., Wei, S., Zhu, M., Song, J., and Peng, P. a.: Comprehensive characterization of humic-like
590 substances in smoke $PM_{2.5}$ emitted from the combustion of biomass materials and fossil fuels, Atmos. Chem.
591 Phys., 16, 13321-13340, 2016.
592 Fang, T., Guo, H., Verma, V., Peltier, R., and Weber, R.: $PM_{2.5}$ water-soluble elements in the southeastern
593 United States: automated analytical method development, spatiotemporal distributions, source
594 apportionment, and implications for heath studies, Atmos. Chem. Phys., 15, 11667-11682, 2015.
595 Fang, T., Verma, V., Bates, J. T., Abrams, J., Klein, M., Strickland, M. J., Sarnat, S. E., Chang, H. H.,
596 Mulholland, J. A., and Tolbert, P. E.: Oxidative potential of ambient water-soluble $PM_{2.5}$ in the southeastern
597 United States: contrasts in sources and health associations between ascorbic acid (AA) and dithiothreitol
598 (DTT) assays, Atmos. Chem. Phys., 16, 3865-3879, 2016.
599 Fang, T., Lakey, P. S. J., Weber, R. J., and Shiraiwa, M.: Oxidative Potential of Particulate Matter and
600 Generation of Reactive Oxygen Species in Epithelial Lining Fluid, Environ. Sci. Technol., 53, 12784-12792,
601 2019.
602 Fang, T., Lakey, P. S. J., Rivera-Rios, J. C., Keutsch, F. N., and Shiraiwa, M.: Aqueous-Phase
603 Decomposition of Isoprene Hydroxy Hydroperoxide and Hydroxyl Radical Formation by Fenton-Like
604 Reactions with Iron Ions, J. Phys. Chem. A, 124, 5230-5236, 2020.

https://doi.org/10.5194/acp-2020-973
Preprint. Discussion started: 20 October 2020

Atmospheric Chemistry and Physics Discussions

Gehling, W., Khachatryan, L., and Dellinger, B.: Hydroxyl radical generation from environmentally persistent free radicals (EPFRs) in $PM_{2.5}$, Environ. Sci. Technol., 48, 4266-4272, 2014.

Gilardoni, S., Massoli, P., Paglione, M., Giulianelli, L., Carbone, C., Rinaldi, M., Decesari, S., Sandrini, S., Costabile, F., and Gobbi, G. P.: Direct observation of aqueous secondary organic aerosol from biomass-burning emissions, Proc. Natl. Acad. Sci. U.S.A., 113, 10013-10018, 2016.

Gligorovski, S., Strekowski, R., Barbati, S., and Vione, D.: Environmental implications of hydroxyl radicals (•OH), Chem. Rev., 115, 13051-13092, 2015.

Goldstein, A. H., Koven, C. D., Heald, C. L., and Fung, I. Y.: Biogenic carbon and anthropogenic pollutants combine to form a cooling haze over the southeastern United States, Proc. Natl. Acad. Sci. U.S.A., 106, 8835-8840, 2009.

Gonzalez, D. H., Cala, C. K., Peng, Q., and Paulson, S. E.: HULIS enhancement of hydroxyl radical formation from Fe(II): Kinetics of fulvic acid–Fe(II) complexes in the presence of lung antioxidants, Environ. Sci. Technol., 51, 7676-7685, 2017.

Graber, E., and Rudich, Y.: Atmospheric HULIS: How humic-like are they? A comprehensive and critical review, Atmos. Chem. Phys., 6, 729-753, 2006.

Hakola, H., Hellén, H., Hemmilä, M., Rinne, J., and Kulmala, M.: In situ measurements of volatile organic compounds in a boreal forest, Atmos. Chem. Phys., 12, 11665-11678, 2012.

Halliwell, B., and Whiteman, M.: Measuring reactive species and oxidative damage in vivo and in cell culture: how should you do it and what do the results mean?, Br. J. Pharmacol., 142, 231-255, 2004.

Hari, P., and Kulmala, M.: Station for Measuring EcosystemsAtmosphere Relations (SMEAR II), Boreal Env. Res., 10, 315-322, 2005.

Hoyle, C. R., Boy, M., Donahue, N. M., Fry, J. L., Glasius, M., Guenther, A., Hallar, A. G., Huff Hartz, K., Petters, M. D., and Petäjä, T.: A review of the anthropogenic influence on biogenic secondary organic aerosol, Atmos. Chem. Phys., 11, 321-343, 2011.

Huang, G., Liu, Y., Shao, M., Li, Y., Chen, Q., Zheng, Y., Wu, Z., Liu, Y., Wu, Y., Hu, M., Li, X., Lu, S., Wang, C., Liu, J., Zheng, M., and Zhu, T.: Potentially Important Contribution of Gas-Phase Oxidation of Naphthalene and Methylnaphthalene to Secondary Organic Aerosol during Haze Events in Beijing, Environ. Sci. Technol., 53, 1235-1244, 2019.

Huang, R.-J., Zhang, Y., Bozzetti, C., Ho, K.-F., Cao, J.-J., Han, Y., Daellenbach, K. R., Slowik, J. G., Platt, S. M., and Canonaco, F.: High secondary aerosol contribution to particulate pollution during haze events in China, Nature, 514, 218-222, 2014.

Jacob, D. J.: Heterogeneous chemistry and tropospheric ozone, Atmos. Environ., 34, 2131-2159, 2000.

Jimenez, J. L., Canagaratna, M., Donahue, N., Prevot, A., Zhang, Q., Kroll, J. H., DeCarlo, P. F., Allan, J. D., Coe, H., and Ng, N.: Evolution of organic aerosols in the atmosphere, Science, 326, 1525-1529, 2009.

https://doi.org/10.5194/acp-2020-973
Preprint. Discussion started: 20 October 2020

Atmospheric Chemistry and Physics Discussions

639 Jin, L., Xie, J., Wong, C. K., Chan, S. K., Abbaszade, G. l., Schnelle-Kreis, J. r., Zimmermann, R., Li, J.,
640 Zhang, G., and Fu, P.: Contributions of city-specific fine particulate matter ($PM_{2.5}$) to differential in vitro
641 oxidative stress and toxicity implications between Beijing and Guangzhou of China, Environ. Sci. Technol.,
642 53, 2881-2891, 2019.
643 Kalyanaraman, B., Darley-Usmar, V., Davies, K. J., Dennery, P. A., Forman, H. J., Grisham, M. B., Mann,
644 G. E., Moore, K., Roberts II, L. J., and Ischiropoulos, H.: Measuring reactive oxygen and nitrogen species
645 with fluorescent probes: challenges and limitations, Free Radic. Biol. Med., 52, 1-6, 2012.
646 Kang, E., Root, M., Toohey, D., and Brune, W. H.: Introducing the concept of potential aerosol mass (PAM),
647 Atmos. Chem. Phys., 7, 5727-5744, 2007.
648 Kehrer, J. P.: The Haber–Weiss reaction and mechanisms of toxicity, Toxicology, 149, 43-50, 2000.
649 Khachatryan, L., Vejerano, E., Lomnicki, S., and Dellinger, B.: Environmentally persistent free radicals
650 (EPFRs). 1. Generation of reactive oxygen species in aqueous solutions, Environ. Sci. Technol., 45, 8559-
651 8566, 2011.
652 Koch, B., and Dittmar, T.: From mass to structure: An aromaticity index for high‐resolution mass data of
653 natural organic matter, Rapid Commun. Mass Spectrom., 20, 926-932, 2006.
654 Kostić, I., Anđelković, T., Nikolić, R., Bojić, A., Purenović, M., Blagojević, S., and Anđelković, D.:
655 Copper(II) and lead(II) complexation by humic acid and humic-like ligands, J. Serb. Chem. Soc., 76, 1325-
656 1336, 2011.
657 Kourtchev, I., Giorio, C., Manninen, A., Wilson, E., Mahon, B., Aalto, J., Kajos, M., Venables, D.,
658 Ruuskanen, T., and Levula, J.: Enhanced volatile organic compounds emissions and organic aerosol mass
659 increase the oligomer content of atmospheric aerosols, Sci. Rep., 6, 35038, 2016.
660 Krapf, M., El Haddad, I., Bruns, E. A., Molteni, U., Daellenbach, K. R., Prévôt, A. S., Baltensperger, U.,
661 and Dommen, J.: Labile peroxides in secondary organic aerosol, Chem, 1, 603-616, 2016.
662 Kuang, X. M., Scott, J. A., da Rocha, G. O., Betha, R., Price, D. J., Russell, L. M., Cocker, D. R., and
663 Paulson, S. E.: Hydroxyl radical formation and soluble trace metal content in particulate matter from
664 renewable diesel and ultra low sulfur diesel in at-sea operations of a research vessel, Aerosol Sci. Technol.,
665 51, 147-158, 2017.
666 Laakso, L., Hussein, T., Aarnio, P., Komppula, M., Hiltunen, V., Viisanen, Y., and Kulmala, M.: Diurnal
667 and annual characteristics of particle mass and number concentrations in urban, rural and Arctic
668 environments in Finland, Atmos. Environ., 37, 2629-2641, 2003.
669 Laglera, L. M., and van den Berg, C. M.: Evidence for geochemical control of iron by humic substances in
670 seawater, Limnol. Oceanogr., 54, 610-619, 2009.

https://doi.org/10.5194/acp-2020-973
Preprint. Discussion started: 20 October 2020

Atmospheric Chemistry and Physics Discussions

671 Lakey, P. S., Berkemeier, T., Tong, H., Arangio, A. M., Lucas, K., Pöschl, U., and Shiraiwa, M.: Chemical
672 exposure-response relationship between air pollutants and reactive oxygen species in the human respiratory
673 tract, Sci. Rep., 6, 32916, 2016.
674 Landreman, A. P., Shafer, M. M., Hemming, J. C., Hannigan, M. P., and Schauer, J. J.: A macrophage-
675 based method for the assessment of the reactive oxygen species (ROS) activity of atmospheric particulate
676 matter (PM) and application to routine (daily-24 h) aerosol monitoring studies, Aerosol Sci. Technol., 42,
677 946-957, 2008.
678 Lelieveld, J., and Pöschl, U.: Chemists can help to solve the air-pollution health crisis, Nature, 551, 291-
679 293, 2017.
680 Li, N., Xia, T., and Nel, A. E.: The role of oxidative stress in ambient particulate matter-induced lung
681 diseases and its implications in the toxicity of engineered nanoparticles, Free Radic. Biol. Med., 44, 1689-
682 1699, 2008.
683 Li, X., Kuang, X. M., Yan, C., Ma, S., Paulson, S. E., Zhu, T., Zhang, Y., and Zheng, M.: Oxidative
684 potential by $PM_{2.5}$ in the North China Plain: generation of hydroxyl radical, Environ. Sci. Technol., 53,
685 512-520, 2018.
686 Lin, M., and Yu, J. Z.: Assessment of interactions between transition metals and atmospheric organics:
687 Ascorbic Acid Depletion and Hydroxyl Radical Formation in Organic-metal Mixtures, Environ. Sci.
688 Technol., 54, 1431−1442, 2020.
689 Lin, P., and Yu, J. Z.: Generation of reactive oxygen species mediated by humic-like substances in
690 atmospheric aerosols, Environ. Sci. Technol., 45, 10362-10368, 2011.
691 Lin, Y., Ma, Y., Qiu, X., Li, R., Fang, Y., Wang, J., Zhu, Y., and Hu, D.: Sources, transformation, and
692 health implications of PAHs and their nitrated, hydroxylated, and oxygenated derivatives in $PM_{2.5}$ in Beijing,
693 J. Geophys. Res. Atmos., 120, 7219-7228, 2015.
694 Liu, F., Saavedra, M. G., Champion, J. A., Griendling, K. K., and Ng, N. L.: Prominent Contribution of
695 Hydrogen Peroxide to Intracellular Reactive Oxygen Species Generated upon Exposure to Naphthalene
696 Secondary Organic Aerosols, Environ. Sci. Technol. Lett., 7, 171-177, 2020.
697 Liu, Q., Baumgartner, J., Zhang, Y., Liu, Y., Sun, Y., and Zhang, M.: Oxidative potential and inflammatory
698 impacts of source apportioned ambient air pollution in Beijing, Environ. Sci. Technol., 48, 12920-12929,
699 2014.
700 Ma, Y., Cheng, Y., Qiu, X., Cao, G., Fang, Y., Wang, J., Zhu, T., Yu, J., and Hu, D.: Sources and oxidative
701 potential of water-soluble humic-like substances (HULIS WS) in fine particulate matter ($PM_{2.5}$) in Beijing,
702 Atmos. Chem. Phys., 18, 5607-5617, 2018.

https://doi.org/10.5194/acp-2020-973
Preprint. Discussion started: 20 October 2020


Atmospheric Chemistry and Physics Discussions

703 Maenhaut, W., Nava, S., Lucarelli, F., Wang, W., Chi, X., and Kulmala, M.: Chemical composition, impact
704 from biomass burning, and mass closure for $PM_{2.5}$ and PM_{10} aerosols at Hyytiälä, Finland, in summer 2007,
705 X-Ray Spectrom., 40, 168-171, 2011.
706 Molina, C., Toro, R., Manzano, C., Canepari, S., Massimi, L., and Leiva-Guzmán, M. A.: Airborne aerosols
707 and human health: Leapfrogging from mass concentration to oxidative potential, Atmosphere, 11, 917,
708 2020.
709 Møller, P., Jacobsen, N. R., Folkmann, J. K., Danielsen, P. H., Mikkelsen, L., Hemmingsen, J. G., Vesterdal,
710 L. K., Forchhammer, L., Wallin, H., and Loft, S.: Role of oxidative damage in toxicity of particulates, Free
711 Radic. Res., 44, 1-46, 2010.
712 Nel, A.: Air pollution-related illness: effects of particles, Science, 308, 804-806, 2005.
713 Ohyama, M., Otake, T., Adachi, S., Kobayashi, T., and Morinaga, K.: A comparison of the production of
714 reactive oxygen species by suspended particulate matter and diesel exhaust particles with macrophages,
715 Inhal. Toxicol., 19, 157-160, 2007.
716 Page, S. E., Sander, M., Arnold, W. A., and McNeill, K.: Hydroxyl radical formation upon oxidation of
717 reduced humic acids by oxygen in the dark, Environ. Sci. Technol., 46, 1590-1597, 2012.
718 Park, J., Park, E. H., Schauer, J. J., Yi, S.-M., and Heo, J.: Reactive oxygen species (ROS) activity of
719 ambient fine particles ($PM_{2.5}$) measured in Seoul, Korea, Environ. Int., 117, 276-283, 2018.
720 Pöschl, U., and Shiraiwa, M.: Multiphase chemistry at the atmosphere–biosphere interface influencing
721 climate and public health in the anthropocene, Chem. Rev., 115, 4440-4475, 2015.
722 Pye, H. O., D'Ambro, E. L., Lee, B. H., Schobesberger, S., Takeuchi, M., Zhao, Y., Lopez-Hilfiker, F., Liu,
723 J., Shilling, J. E., and Xing, J.: Anthropogenic enhancements to production of highly oxygenated molecules
724 from autoxidation, Proc. Natl. Acad. Sci. U.S.A., 116, 6641-6646, 2019.
725 Qiu, J., Liang, Z., Tonokura, K., Colussi, A. J., and Enami, S.: Stability of Monoterpene-Derived α-
726 Hydroxyalkyl-Hydroperoxides in Aqueous Organic Media: Relevance to the Fate of Hydroperoxides in
727 Aerosol Particle Phases, Environ. Sci. Technol., 54, 3890-3899, 2020.
728 Qu, J., Li, Y., Zhong, W., Gao, P., and Hu, C.: Recent developments in the role of reactive oxygen species
729 in allergic asthma, J. Thorac. Dis., 9, E32, 2017.
730 Rao, X., Zhong, J., Brook, R. D., and Rajagopalan, S.: Effect of particulate matter air pollution on
731 cardiovascular oxidative stress pathways, Antioxid. Redox. Signal., 28, 797-818, 2018.
732 Reinmuth-Selzle, K., Kampf, C. J., Lucas, K., Lang-Yona, N., Fröhlich-Nowoisky, J., Shiraiwa, M., Lakey,
733 P. S., Lai, S., Liu, F., and Kunert, A. T.: Air pollution and climate change effects on allergies in the
734 anthropocene: abundance, interaction, and modification of allergens and adjuvants, Environ. Sci. Technol.,
735 51, 4119-4141, 2017.

https://doi.org/10.5194/acp-2020-973
Preprint. Discussion started: 20 October 2020


Atmospheric Chemistry and Physics Discussions

736 Scheinhardt, S., Müller, K., Spindler, G., and Herrmann, H.: Complexation of trace metals in size-
737 segregated aerosol particles at nine sites in Germany, Atmos. Environ., 74, 102-109, 2013.
738 Shi, Y., Dai, Y., Liu, Z., Nie, X., Zhao, S., Zhang, C., and Jia, H.: Light-induced variation in
739 environmentally persistent free radicals and the generation of reactive radical species in humic substances,
740 Front. Environ. Sci. Eng., 14, 1-10, 2020.
741 Shiraiwa, M., Ueda, K., Pozzer, A., Lammel, G., Kampf, C. J., Fushimi, A., Enami, S., Arangio, A. M.,
742 Fröhlich-Nowoisky, J., Fujitani, Y., Furuyama, A., Lakey, P. S. J., Lelieveld, J., Lucas, K., Morino, Y.,
743 Pöschl, U., Takahama, S., Takami, A., Tong, H., Weber, B., Yoshino, A., and Sato, K.: Aerosol health
744 effects from molecular to global scales, Environ. Sci. Technol., 51, 13545-13567, 2017.
745 Shrivastava, M., Andreae, M. O., Artaxo, P., Barbosa, H. M., Berg, L. K., Brito, J., Ching, J., Easter, R. C.,
746 Fan, J., and Fast, J. D.: Urban pollution greatly enhances formation of natural aerosols over the Amazon
747 rainforest, Nat. Commun., 10, 1046, 2019.
748 Sies, H., Berndt, C., and Jones, D. P.: Oxidative stress, Annu. Rev. Biochem., 86, 715-748, 2017.
749 Singh, D. K., and Gupta, T.: Role of transition metals with water soluble organic carbon in the formation
750 of secondary organic aerosol and metallo - organics in PM_1 sampled during post monsoon and pre-winter
751 time, J. Aerosol Sci., 94, 56-69, 2016.
752 Tang, W.-W., Zeng, G.-M., Gong, J.-L., Liang, J., Xu, P., Zhang, C., and Huang, B.-B.: Impact of
753 humic/fulvic acid on the removal of heavy metals from aqueous solutions using nanomaterials: a review,
754 Sci. Total Environ., 468, 1014-1027, 2014.
755 Tong, H., Arangio, A. M., Lakey, P. S., Berkemeier, T., Liu, F., Kampf, C. J., Brune, W. H., Pöschl, U.,
756 and Shiraiwa, M.: Hydroxyl radicals from secondary organic aerosol decomposition in water, Atmos. Chem.
757 Phys., 16, 1761-1771, 2016a.
758 Tong, H., Kourtchev, I., Pant, P., Keyte, I. J., O'Connor, I. P., Wenger, J. C., Pope, F. D., Harrison, R. M.,
759 and Kalberer, M.: Molecular composition of organic aerosols at urban background and road tunnel sites
760 using ultra-high resolution mass spectrometry, Faraday Discuss., 189, 51-68, 2016b.
761 Tong, H., Lakey, P. S., Arangio, A. M., Socorro, J., Kampf, C. J., Berkemeier, T., Brune, W. H., Pöschl,
762 U., and Shiraiwa, M.: Reactive oxygen species formed in aqueous mixtures of secondary organic aerosols
763 and mineral dust influencing cloud chemistry and public health in the Anthropocene, Faraday Discuss., 200,
764 251-270, 2017.
765 Tong, H., Lakey, P. S., Arangio, A. M., Socorro, J., Shen, F., Lucas, K., Brune, W. H., Pöschl, U., and
766 Shiraiwa, M.: Reactive oxygen species formed by secondary organic aerosols in water and surrogate lung
767 fluid, Environ. Sci. Technol., 52, 11642-11651, 2018.
768 Tong, H., Zhang, Y., Filippi, A., Wang, T., Li, C., Liu, F., Leppla, D., Kourtchev, I., Wang, K., Keskinen,
769 H.-M., Levula, J. T., Arangio, A. M., Shen, F., Ditas, F., Martin, S. T., Artaxo, P., Godoi, R. H. M.,

https://doi.org/10.5194/acp-2020-973
Preprint. Discussion started: 20 October 2020

Atmospheric Chemistry and Physics Discussions

770 Yamamoto, C. I., Souza, R. A. F. d., Huang, R.-J., Berkemeier, T., Wang, Y., Su, H., Cheng, Y., Pope, F.
771 D., Fu, P., Yao, M., Pöhlker, C., Petäjä, T., Kulmala, M., Andreae, M. O., Shiraiwa, M., Pöschl, U.,
772 Hoffmann, T., and Kalberer, M.: Radical Formation by Fine Particulate Matter Associated with Highly
773 Oxygenated Molecules, Environ. Sci. Technol., 53, 12506-12518, 2019.
774 Tröstl, J., Chuang, W. K., Gordon, H., Heinritzi, M., Yan, C., Molteni, U., Ahlm, L., Frege, C., Bianchi, F.,
775 and Wagner, R.: The role of low-volatility organic compounds in initial particle growth in the atmosphere,
776 Nature, 533, 527-531, 2016.
777 Tseitlin, M., Eaton, S. S., and Eaton, G. R.: Uncertainty analysis for absorption and first‐derivative
778 electron paramagnetic resonance spectra, Concepts Magn. Reson., Part A, 40, 295-305, 2012.
779 Valavanidis, A., Fiotakis, K., Bakeas, E., and Vlahogianni, T.: Electron paramagnetic resonance study of
780 the generation of reactive oxygen species catalysed by transition metals and quinoid redox cycling by
781 inhalable ambient particulate matter, Redox. Rep., 10, 37-51, 2005.
782 Verma, V., Fang, T., Guo, H., King, L., Bates, J., Peltier, R., Edgerton, E., Russell, A., and Weber, R.:
783 Reactive oxygen species associated with water-soluble $PM_{2.5}$ in the southeastern United States:
784 spatiotemporal trends and source apportionment, Atmos. Chem. Phys., 14, 12915-12930, 2014.
785 Verma, V., Fang, T., Xu, L., Peltier, R. E., Russell, A. G., Ng, N. L., and Weber, R. J.: Organic aerosols
786 associated with the generation of reactive oxygen species (ROS) by water-soluble $PM_{2.5}$, Environ. Sci.
787 Technol., 49, 4646-4656, 2015.
788 Wang, C., Wang, Z., Peng, A., Hou, J., and Xin, W.: Interaction between fulvic acids of different origins
789 and active oxygen radicals, Sci. China C Life Sci., 39, 267-275, 1996.
790 Wang, K., Zhang, Y., Huang, R.-J., Cao, J., and Hoffmann, T.: UHPLC-Orbitrap mass spectrometric
791 characterization of organic aerosol from a central European city (Mainz, Germany) and a Chinese megacity
792 (Beijing), Atmos. Environ., 189, 22-29, 2018a.
793 Wang, K., Zhang, Y., Huang, R.-J., Wang, M., Ni, H., Kampf, C. J., Cheng, Y., Bilde, M., Glasius, M., and
794 Hoffmann, T.: Molecular characterization and source identification of atmospheric particulate
795 organosulfates using ultrahigh resolution mass spectrometry, Environ. Sci. Technol., 53, 6192-6202, 2019.
796 Wang, N., Miller, C. J., Wang, P., and Waite, T. D.: Quantitative determination of trace hydrogen peroxide
797 in the presence of sulfide using the Amplex Red/horseradish peroxidase assay, Anal. Chim. Acta, 963, 61-
798 67, 2017.
799 Wang, S., Ye, J., Soong, R., Wu, B., Yu, L., Simpson, A. J., and Chan, A. W.: Relationship between
800 chemical composition and oxidative potential of secondary organic aerosol from polycyclic aromatic
801 hydrocarbons, Atmos. Chem. Phys., 18, 3987-4003, 2018b.

https://doi.org/10.5194/acp-2020-973
Preprint. Discussion started: 20 October 2020

802 Wang, Y., Arellanes, C., Curtis, D. B., and Paulson, S. E.: Probing the source of hydrogen peroxide
803 associated with coarse mode aerosol particles in Southern California, Environ. Sci. Technol., 44, 4070-
804 4075, 2010.
805 Wang, Y., Hopke, P. K., Sun, L., Chalupa, D. C., and Utell, M. J.: Laboratory and field testing of an
806 automated atmospheric particle-bound reactive oxygen species sampling-analysis system, J. Toxicol., 2011,
807 419476, 2011a.
808 Wang, Y., Kim, H., and Paulson, S. E.: Hydrogen peroxide generation from α-and β-pinene and toluene
809 secondary organic aerosols, Atmos. Environ., 45, 3149-3156, 2011b.
810 Wang, Y., Arellanes, C., and Paulson, S. E.: Hydrogen peroxide associated with ambient fine-mode, diesel,
811 and biodiesel aerosol particles in Southern California, Aerosol Sci. Technol., 46, 394-402, 2012.
812 Wang, Y., Hu, M., Guo, S., Wang, Y., Zheng, J., Yang, Y., Zhu, W., Tang, R., Li, X., and Liu, Y.: The
813 secondary formation of organosulfates under interactions between biogenic emissions and anthropogenic
814 pollutants in summer in Beijing, Atmos. Chem. Phys., 18, 10693-10713, 2018c.
815 Wei, J., Yu, H., Wang, Y., and Verma, V.: Complexation of Iron and Copper in Ambient Particulate Matter
816 and Its Effect on the Oxidative Potential Measured in a Surrogate Lung Fluid, Environ. Sci. Technol., 53,
817 1661-1671, 2019.
818 Win, M. S., Tian, Z., Zhao, H., Xiao, K., Peng, J., Shang, Y., Wu, M., Xiu, G., Lu, S., and Yonemochi, S.:
819 Atmospheric HULIS and its ability to mediate the reactive oxygen species (ROS): A review, J. Environ.
820 Sci., 71, 13-31, 2018.
821 Xia, T., Korge, P., Weiss, J. N., Li, N., Venkatesen, M. I., Sioutas, C., and Nel, A.: Quinones and aromatic
822 chemical compounds in particulate matter induce mitochondrial dysfunction: implications for ultrafine
823 particle toxicity, Environ. Health Perspect., 112, 1347-1358, 2004.
824 Xiong, Q., Yu, H., Wang, R., Wei, J., and Verma, V.: Rethinking dithiothreitol-based particulate matter
825 oxidative potential: measuring dithiothreitol consumption versus reactive oxygen species generation,
826 Environ. Sci. Technol., 51, 6507-6514, 2017.
827 Xu, L., Guo, H., Boyd, C. M., Klein, M., Bougiatioti, A., Cerully, K. M., Hite, J. R., Isaacman-VanWertz,
828 G., Kreisberg, N. M., and Knote, C.: Effects of anthropogenic emissions on aerosol formation from isoprene
829 and monoterpenes in the southeastern United States, Proc. Natl. Acad. Sci. U.S.A., 112, 37-42, 2015.
830 Yan, D., Cui, H., Zhu, W., Talbot, A., Zhang, L. G., Sherman, J. H., and Keidar, M.: The strong cell-based
831 hydrogen peroxide generation triggered by cold atmospheric plasma, Sci. Rep., 7, 1-9, 2017.
832 Yang, R., Su, H., Qu, S., and Wang, X.: Capacity of humic substances to complex with iron at different
833 salinities in the Yangtze River estuary and East China Sea, Sci. Rep., 7, 1381, 2017.

https://doi.org/10.5194/acp-2020-973
Preprint. Discussion started: 20 October 2020

Atmospheric Chemistry and Physics Discussions

834 Yassine, M. M., Harir, M., Dabek‐Zlotorzynska, E., and Schmitt‐Kopplin, P.: Structural characterization
835 of organic aerosol using Fourier transform ion cyclotron resonance mass spectrometry: aromaticity
836 equivalent approach, Rapid Commun. Mass Spectrom., 28, 2445-2454, 2014.
837 Yu, H., Wei, J., Cheng, Y., Subedi, K., and Verma, V.: Synergistic and antagonistic interactions among the
838 particulate matter components in generating reactive oxygen species based on the dithiothreitol assay,
839 Environ. Sci. Technol., 52, 2261-2270, 2018.
840 Zhang, Y., and Tao, S.: Global atmospheric emission inventory of polycyclic aromatic hydrocarbons (PAHs)
841 for 2004, Atmos. Environ., 43, 812-819, 2009.
842 Zhao, H., Joseph, J., Zhang, H., Karoui, H., and Kalyanaraman, B.: Synthesis and biochemical applications
843 of a solid cyclic nitrone spin trap: a relatively superior trap for detecting superoxide anions and glutathiyl
844 radicals, Free Radic. Biol. Med., 31, 599-606, 2001.
845 Zhou, J., Zotter, P., Bruns, E. A., Stefenelli, G., Bhattu, D., Brown, S., Bertrand, A., Marchand, N.,
846 Lamkaddam, H., and Slowik, J. G.: Particle-bound reactive oxygen species (PB-ROS) emissions and
847 formation pathways in residential wood smoke under different combustion and aging conditions, Atmos.
848 Chem. Phys., 18, 6985-7000, 2018.
849 Zuo, Y., and Hoigne, J.: Formation of hydrogen peroxide and depletion of oxalic acid in atmospheric water
850 by photolysis of iron(III)-oxalato complexes, Environ. Sci. Technol., 26, 1014-1022, 1992.

851

https://doi.org/10.5194/acp-2020-973
Preprint. Discussion started: 20 October 2020


Atmospheric Chemistry and Physics Discussions

852 ***Data availability***

853 The dataset for this paper is available upon request from the corresponding author (h.tong@mpic.de).

854 ***Supporting Information***

855 Supporting material consists of seven figures and five tables.

856 ***Author contributions***

857 HT and UP designed the esperiment and wrote up the original draft together with FL. CX, SY, and HK
858 involved in the collection of ambient particles. HT, FL, AF, and YZ particpated in laboratory measurements
859 and data analysis. All other co-authors participated in results discussion and manuscript editing.

860 ***AUTHOR INFORMATION***

861 ***Corresponding Author***

862 *Haijie Tong*

863 Phone (+49) 6131-305-7040

864 E-mail: h.tong@mpic.de;

865 ***ORCID***:

866 Haijie Tong: 0000-0001-9887-7836

867 Maosheng Yao: 0000-0002-1442-8054

868 Thomas Berkemeier: 0000-0001-6390-6465

869 Manabu Shiraiwa: 0000-0003-2532-5373

870 Ulrich Pöschl: 0000-0003-1412-35570000-0001-9887-7836

871 ***Competing interests***

872 The authors declare no competing financial interest.

873 ***Acknowledgements***

https://doi.org/10.5194/acp-2020-973
Preprint. Discussion started: 20 October 2020

Atmospheric Chemistry and Physics Discussions

874 This work was funded by the Max Planck Society, ACTRIS, ECAC, the Finnish Centre of Excellence under
875 Academy of Finland (projects no. 307331 and 272041). Siegfried Herrmann and Steve Galer from Climate
876 Geochemistry Department of Max Planck Institute for Chemistry are gratefully acknowledged for ICP-MS
877 analysis. Technical staffs at SMEARII station are acknowledged for the impactor maintenance. MS
878 acknowledges funding from the National Science Foundation (CHE-1808125) and the Japan Society for
879 the Promotion of Science (JSPS; No. 16K12582).

https://doi.org/10.5194/acp-2020-973
Preprint. Discussion started: 20 October 2020

Atmospheric Chemistry and Physics Discussions

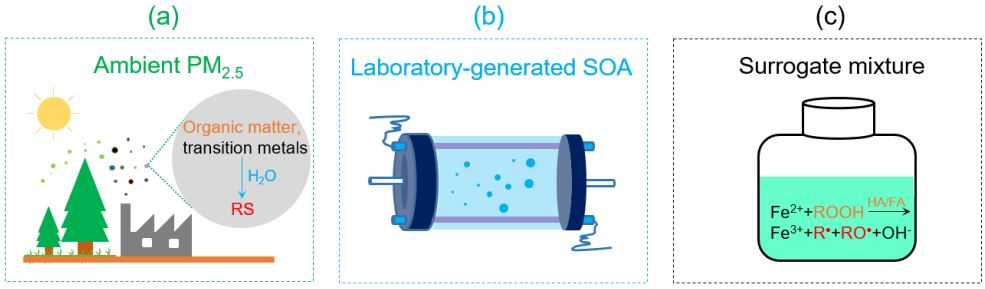

Figure 1. Schematic illustration of research approach and comparison of reactive species (RS) formed upon interaction of water with ambient fine particulate matter ($PM_{2.5}$), with laboratory generated secondary organic aerosols (SOA), and in surrogate mixtures. ROOH: organic hydroperoxide. HA: humic acid. FA: fulvic acid. $R^{\bullet}$ and $RO^{\bullet}$: C- and O-centered organic radicals, respectively.

https://doi.org/10.5194/acp-2020-973
Preprint. Discussion started: 20 October 2020

Atmospheric Chemistry and Physics Discussions

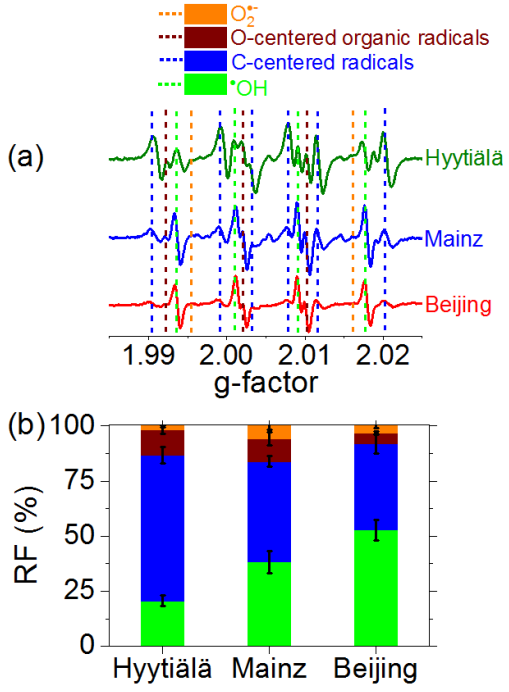

Figure 2. (a) EPR spectra and (b) relative fractions (RF) of different types of radicals formed in aqueous extracts of ambient $PM_{2.5}$ from Hyytiälä, Mainz, and Beijing. Dotted vertical lines in (a) indicate peak positions of different radical adducts. The spectra intensity in (a), RF values and error bars in (b) represent arithmetic mean values and standard error (6-13 samples per location).

https://doi.org/10.5194/acp-2020-973
Preprint. Discussion started: 20 October 2020

Atmospheric Chemistry and Physics Discussions

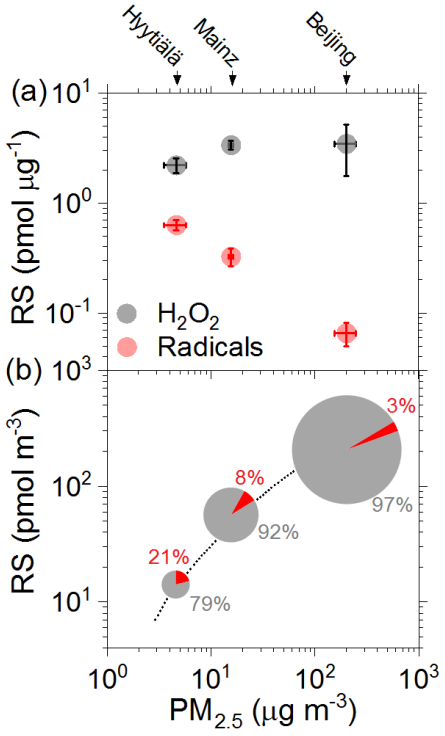

Figure 3. (a) Mass-specific yield and (b) air sample volume-specific yield of radicals (●) and H_2O_2 (●) observed upon water interaction of fine $PM_{2.5}$ from Hyytiälä, Mainz, and Beijing plotted against $PM_{2.5}$ concentration. The error bars represent standard errors of the mean (4-12 samples per location). The dotted line and pie charts are to guide the eye, reflecting the increase of total air sample volume-specific RS yield (not to scale) and the relative contributions of H_2O_2 and radicals.

https://doi.org/10.5194/acp-2020-973
Preprint. Discussion started: 20 October 2020

Atmospheric Chemistry and Physics Discussions

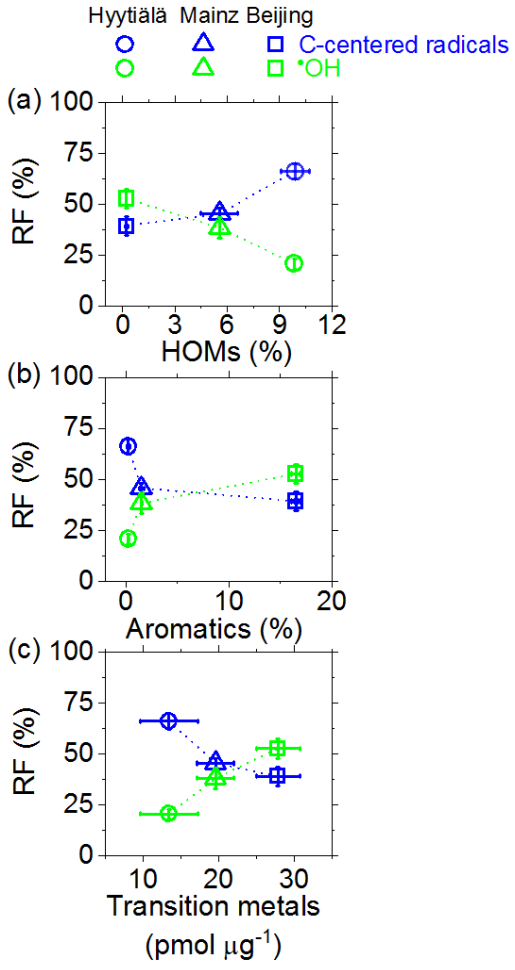

896

897 **Figure 4.** Correlation of (a) highly oxygenated organic molecules (HOMs), (b) aromatics, and (c) water-
898 soluble transition metals in ambient $PM_{2.5}$ with relative fractions (RF) of R• and •OH observed upon
899 interaction with water. The relative abundances of HOMs and aromatics in (a-b) represent the sum
900 chromatographic area of HOMs or aromatics divided by the sum chromatographic area of all assigned
901 organic compounds. The abundances of HOMs in (a) were adopted from a recent companion study (Tong
902 et al., 2019). The error bars represent standard errors of the mean (4 to 12 samples per location). The dashed
903 lines are to guide the eye.

https://doi.org/10.5194/acp-2020-973
Preprint. Discussion started: 20 October 2020

Atmospheric Chemistry and Physics Discussions

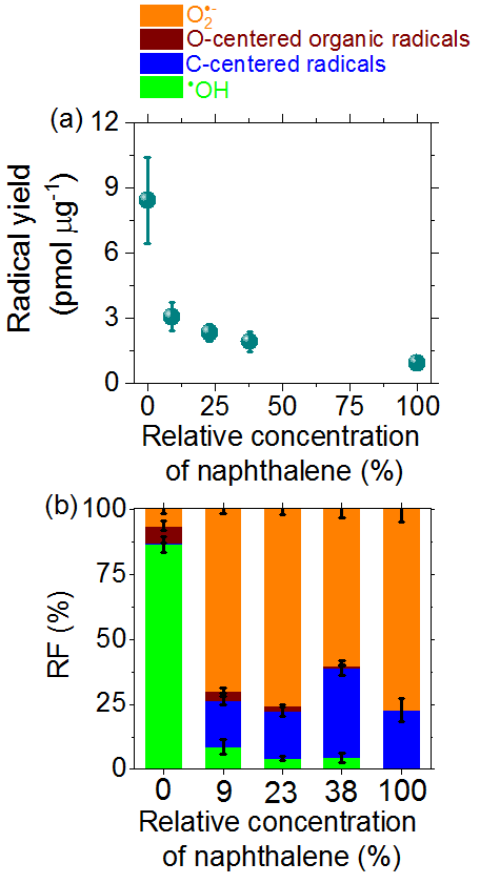

Figure 5. (a) Mass-specific yields and (b) relative fractions (RF) of radicals formed upon aqueous extraction of laboratory-generated SOA from different precursors. The relative concentration of naphthalene represents the relative molar fraction of gas-phase naphthalene to the mixture of naphthalene and β-pinene. The error bars represent standard errors (4-6 samples per data point).

https://doi.org/10.5194/acp-2020-973
Preprint. Discussion started: 20 October 2020

Atmospheric Chemistry and Physics Discussions

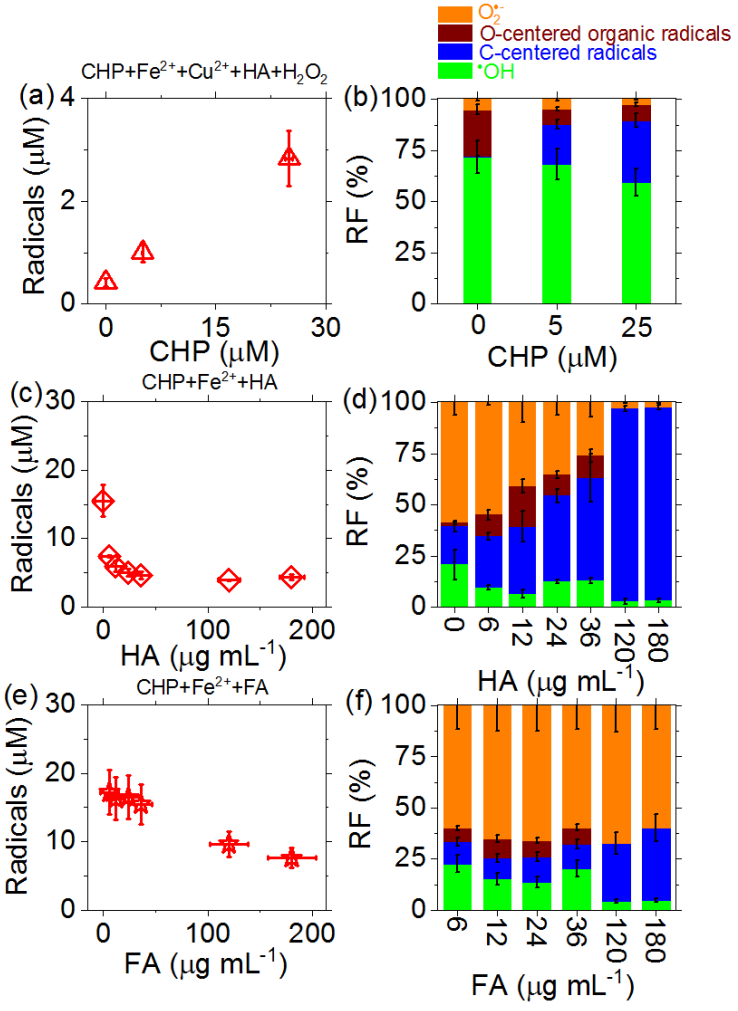

Figure 6. (a, c, e) Total radical yields and (b, d, f) relative fractions (RF) of different radical types observed in aqueous surrogate mixtures of CHP, Fe^{2+}, Cu^{2+}, HA, FA, and H_2O_2. (a, b): 0-25 μM CHP, 43 μM Fe^{2+}, 3 μM Cu^{2+}, 4 μg mL^{-1} HA, 7 μM H_2O_2 (CHP+Fe^{2+}+Cu^{2+}+HA+H_2O_2). (c, d): 100 μM CHP, 300 μM Fe^{2+}, 0-180 μg mL^{-1} HA (CHP+Fe^{2+}+HA). (e, f): 100 μM CHP, 300 μM Fe^{2+}, 6-180 μg mL^{-1} FA (CHP+Fe^{2+}+FA). The error bars represent uncertainties of signal integration of EPR spectra (for y-axis) or experimental uncertainties of the solution concentration (for x-axis). CHP: cumene hydroperoxide. HA: humic acid. FA: fulvic acid.